



Meteorologisk
institutt
met.no

Report 07/03

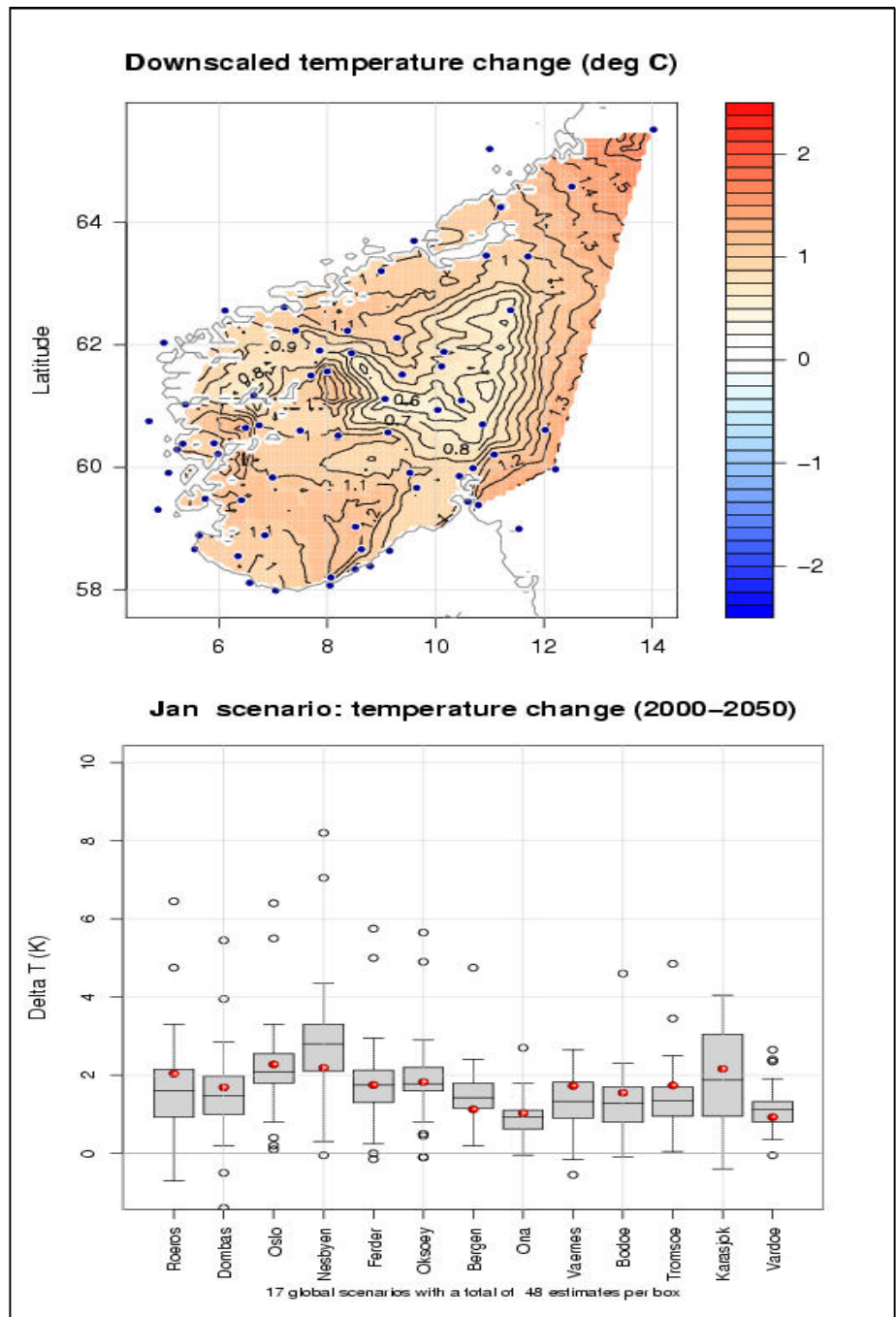
KLIMA

RegClim:
Regional Climate Development
under Global Warming

Reg Clim

Empirical-based refinement of dynamically downscaled temperature scenarios in southern Norway

R. E. Benestad and I. Hanssen-Bauer



met.no REPORT

NORWEGIAN METEOROLOGICAL INSTITUTE
BOX 43 BLINDERN, N - 0313 OSLO, NORWAY

PHONE +47 22 96 30 00

TITLE:

Empirical-based refinement of dynamically downscaled temperature scenarios in southern Norway

AUTHORS:

R.E. Benestad and I. Hanssen-Bauer

PROJECT CONTRACTORS:

The Norwegian Research Council (Contract NRC-No 120656/720 RegClim) and The Norwegian Meteorological Institute

SUMMARY:

Daily temperature scenarios derived through dynamical downscaling have been subject to subsequent empirical downscaling analysis, geographical modelling, and a spatial interpolation. These refined scenarios are compared with the results from the dynamical downscaling.

The empirically and dynamically based results give different results, however, the major difference between the refined scenarios and the temperatures from the dynamical downscaling being the introduction of more prominent small-scale geographical features in the empirical-based analysis. The empirically-based refinement yields somewhat weaker warming in winter, summer and autumn, but slightly stronger warming in spring.

KEYWORDS:

Climate change; empirical downscaling; dynamical downscaling; daily temperature.

SIGNATURES:

.....
Eirik Førland
Principal Investigator

.....
Øystein Hov
Head of **met.no** Climatology Division

ISSN 0805-9918

REPORT NO.
07/03 KLIMA

DATE
2003-06-19

Empirical-based refinement of dynamically downscaled temperature scenarios in southern Norway.

By R.E. Benestad, I. Hanssen-Bauer

*The Norwegian Meteorological Institute, PO Box 43, 0313, Oslo, Norway **

June 19, 2003

ABSTRACT

Daily temperature scenarios derived through dynamical downscaling have been subject to subsequent empirical downscaling analysis, geographical modelling, and a spatial interpolation. These refined scenarios are compared with the results from the dynamical downscaling.

The empirically and dynamically based results give different results, however, the major difference between the refined scenarios and the temperatures from the dynamical downscaling being the introduction of more prominent small-scale geographical features in the empirical-based analysis. The empirically-based refinement yields somewhat weaker warming in winter, summer and autumn, but slightly stronger warming in spring.

KEY WORDS: Climate change empirical downscaling dynamical downscaling daily temperature

** Corresponding author: R.E. Benestad, rasmus.benestad@met.no, The Norwegian Meteorological Institute, PO Box 43, 0313 Oslo, Norway, phone +47-22 96 31 70, fax +47-22 96 30 50*

1 Introduction

Global warming due to anthropogenic emissions of so-called greenhouse gases may introduce changes to our environment, and it is important to assess what changes we can expect. In order to do so, one must employ all available knowledge and the best tools for making climate scenarios. One important approach involves global climate models (GCMs) which have been integrated with prescribed changes to forcing factors such as greenhouse gases. Such models do not give detailed and reliable regional or local scenarios, due to coarse spatial resolution and climate model shortcomings (*IPCC, 2001; Grotch & MacCracken, 1991*). It may nevertheless be possible to extract information about the regional and local climate through the means of downscaling. Two types of downscaling are frequently employed: i) dynamical involving nested regional climate models (RCMs) with higher spatial resolution (*Christensen et al., 2001; Räisänen et al., 1999; Charles et al., 1999; Christensen et al., 1998*) and ii) empirical utilising historically based relationships between large-scale and local variability (*Beckmann & Buishand, 2002; Oshima et al., 2002; Wilby & Wigley, 2000; Easterling, 1999; Zorita & von Storch, 1999; Schubert, 1998; Wilby et al., 1998b; Goodess & Palutikof, 1998; Heyen et al., 1996; von Storch et al., 1993a*). The two different approaches have different strengths and weaknesses, and a comparison between the two methods may give an indication of the confidence associated with the downscaled results. Empirical downscaling may also be used to further refine the results from dynamical downscaling.

Hanssen-Bauer et al. (2003, 2000) have compared monthly mean results from empirical and dynamical downscaling for Norway, and found that the two approaches give similar warming trends along the coast and at elevated localities in the inland. While dynamical downscaling gave rather small trends in the inland the warming projected in winter and spring by empirical downscaling was larger in valleys than on mountains. It was argued that less favourable conditions for ground inversions are consistent with the future projection of increased winter wind speeds and reduced snow-cover, and that the results from empirical downscaling thus are reasonable. The dynamical downscaling model has still too coarse resolution to resolve these inversions.

Hellström et al. (2001) compared dynamical and empirical downscaled results for Sweden, and others have conducted similar type of comparisons for the rest of the world (*Wilby et al., 1998a; Murphy, 2000, 1999; Kidson & Thompson, 1998*). *Hellström et al. (2001)* found that the temporal and spatial variability of precipitation changes are higher in the statistical downscaled scenarios than in corresponding dynamical downscaled ones. *Murphy (1999)* estimated that the overall levels of skill of empirical and dynamical downscaling methods for monthly temperature were similar over Europe, although *Murphy (2000)* reported that the statistically downscaled results tend to be less similar to the GCM output than the RCM results. *Kidson & Thompson (1998)* also found comparable skill between statistically and dynamically downscaled daily and monthly temperature and rainfall in New Zealand.

Skaugen et al. (2002) compared the spatially interpolated mean values from RCM integration of the present-day climate in Norway with corresponding station observations, and found that the RCM may not give sufficiently realistic description of the local climate. The RCM temperature estimates were generally too low, which *Skaugen et al. (2002)* suggested could be due to an unrealistically smooth model topography. Furthermore, they also stated that the RCM description of the winter temperature may not account adequately for ground inversion. *Skaugen et al. (2002)* investigated various methods for correcting the RCM bias in both precipitation and temperature. A linear regression ($T' = aT + b$) was tried for correcting the temperature (T), but *Skaugen et al. (2002)* argued that a reduction of variance ($|a| < 1$) would result in under-estimated temperature changes. Instead, a correction based on height only was recommended (mathematically similar to the regression equation, but with $a = 1$).

Here empirical downscaling is applied to dynamically downscaled results in an attempt to improve the description of local climatic features. This study differs from *Skaugen et al. (2002)* by utilising more advanced empirical downscaling models. Furthermore, the year is divided into four seasons (December–February, March–May, June–August, and September–November) whereas *Skaugen et al. (2002)* analysed the 12 calendar months separately (each with a smaller batch of data). We compare the downscaled daily temperature from the dynamical downscaling and the scenarios obtained through further refinement based on empirical downscaling and geographical information.

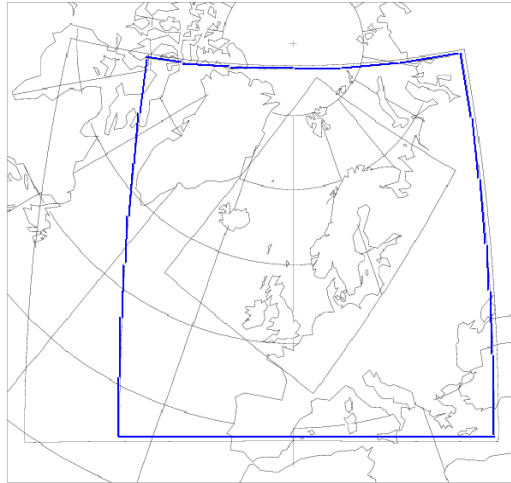


Figure 1. The spatial domain used in the HIRHAM nested modelling (courtesy of Jan Erik Haugen).

2 Methods & Data

The global climate scenarios, from which the downscaled scenarios were derived, were produced with the Max-Planck-Institute's global climate model ECHAM4/OPYC3 (Roeckner et al., 1992; Oberhuber, 1993) GSDIO experiment. This integration follows the IS92a emission scenario (IPCC, 1995), and takes into account the direct and indirect effects of man-made aerosols, as well as tropospheric ozone concentrations. The ECHAM4/OPYC3 model uses so-called flux-correction to ensure a realistic description of the present-day climate.

The dynamical downscaling was carried out with the HIRHAM regional climate model and is described in Hanssen-Bauer et al. (2003); Bjørge et al. (2000); Nordeng et al. (2000); Haugen et al. (2000, 1999a,b); Bjørge & Haugen (1999). The RCM grid has a 55km spatial resolution and the same 19 vertical levels as the driving global climate model. The lateral boundary conditions were pressure, temperature, horizontal velocity, specific humidity, and liquid cloud water at 12-hour intervals taken from the GSDIO experiments*. The geographical boundaries of the HIRHAM RCM are shown in Figure 1 (using the second largest domain shown in blue). The dynamically downscaled results carried out with HIRHAM at the Norwegian Meteorological Institute (DNMI) have been compared with similar work from Danish (DMI) and Swedish (RCA) groups (Christensen et al., 2001). The comparison revealed slightly different projected warming among the different groups, however, it is important to keep in mind that the comparison was made between integrations of different lengths (DMI 8 and 9 years; DNMI 2×20 years; RCA 2×10 years) and some of these differences may be due to sampling fluctuations and internal variability. The temperature scenarios from Bjørge et al. (2000) gave systematically weaker warming than the other groups, possible as a result of different representation of aerosol and ozone forcings in the global climate models.

The empirical downscaling employed in this study is based on a 'common EOF' frame work (Benestad, 2001, 2002a,b) using the December–February, March–May, June–August and September–November daily T(2m) combined observation-model fields respectively. Hence, these results may differ from those from Hanssen-Bauer et al. (2000) because different methodology as well as time periods were used, and here daily averages are used instead of monthly means. Furthermore, the fields used for model calibration were taken from the ECMWF reanalysis (Gibson et al., 1997) (ERA-15) interpolated onto the HIRHAM model grid, whereas the calibration by Hanssen-Bauer used UK Met Office SLP data and temperatures from University of East Anglia (Jones et al., 1998). The common EOFs were produced with the R package called `clim.pact` (Benestad, 2003b,a) (available from <http://cran.r-project.org/>). The

* Assuming the IPCC IS92a emission scenario with observed CO₂ concentrations until 1990 and thereafter assuming a 1% annual increase compounded.

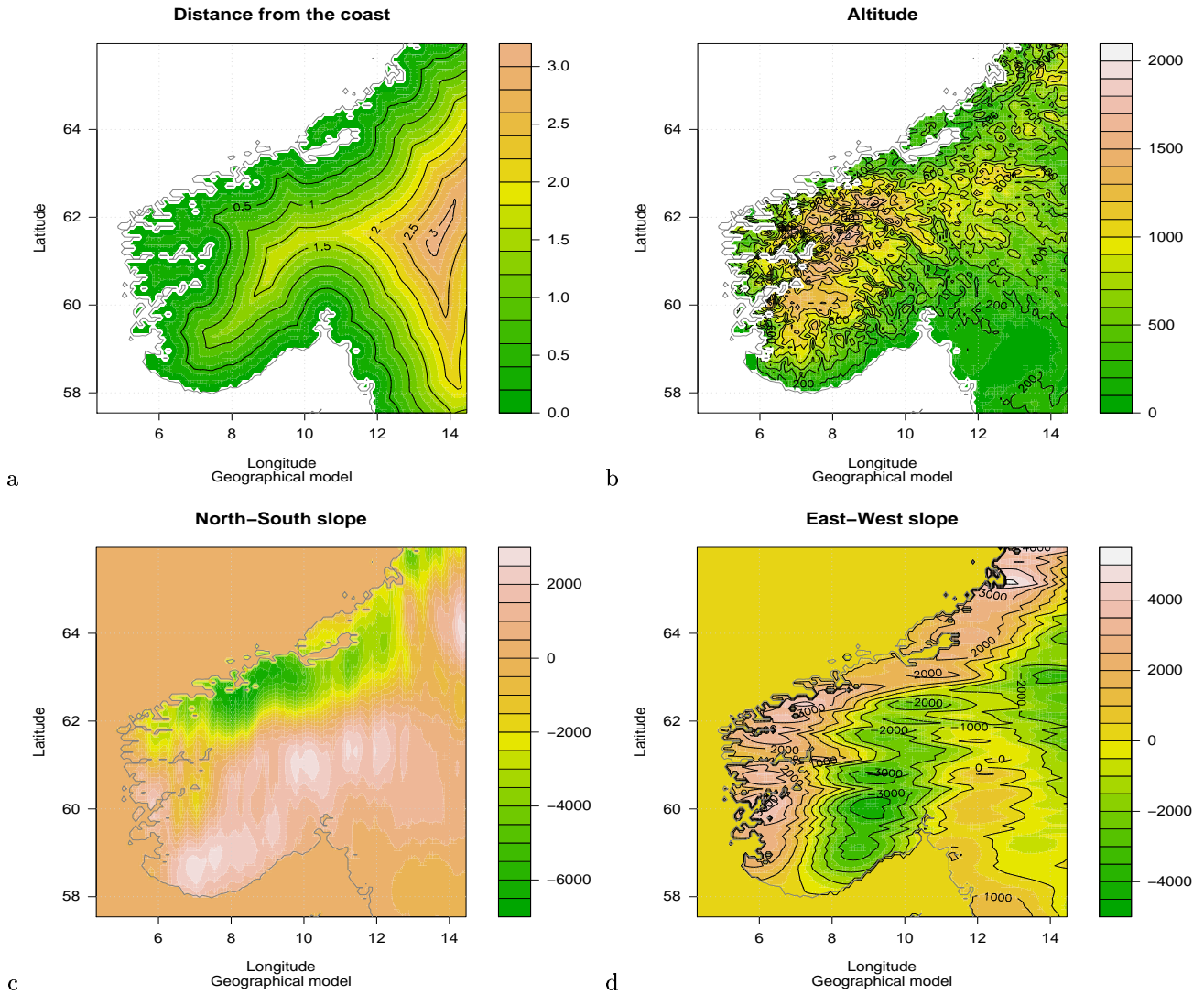


Figure 2. The geographical parameters distance from the coast (a), altitude (b), north-south slope (c) and the east-west slope (d) employed by the geographical model in addition to latitude and longitude.

downscaling employed 2-meter temperature predictors covering: 58°N–70°N 4°E–25°E. The statistical model used for the downscaling consisted of a multiple linear regression with forward-backward stepwise screening. The regression analysis was carried out on daily anomalies, which were computed by subtracting a climatological annual cycle. The annual cycle was estimated by `clim.pact` by fitting the 6 leading harmonics to the time series.

It is well-known that many climatic parameters depend on geographical aspects such as the distance from the coast, altitude, longitude and latitude (*Prudhomme & Reed, 1999; Tveito & Førland, 1999*). In order to produce realistically looking maps of temperature changes, the downscaled results for the temperature stations were spatially interpolated by taking into account these geographical dependencies. The geographical model used for the interpolation is a multiple regression against the six geographical parameters: 1) *distance-from-the-coast* (*dist*), 2) *altitude* (*alt*), 3) *latitude* (*lat*), 4) *longitude* (*lon*), 5) *north-south gradient* (*grad.ns*), and 6) *east-west gradient* (*grad.ew*):

$$\hat{y} = c_0 + c_1 \times \text{dist} + c_2 \times \text{alt} + c_3 \times \text{lat} + c_4 \times \text{lon} + c_5 \times \text{grad.ns} + c_6 \times \text{grad.ew}. \quad (1)$$

Figure 2 shows the geographical distribution of four geographical parameters: *distance from the coast*, *altitude*, *north-south slope* and *east-west slope*, and Figure 3 shows the results from a spatial

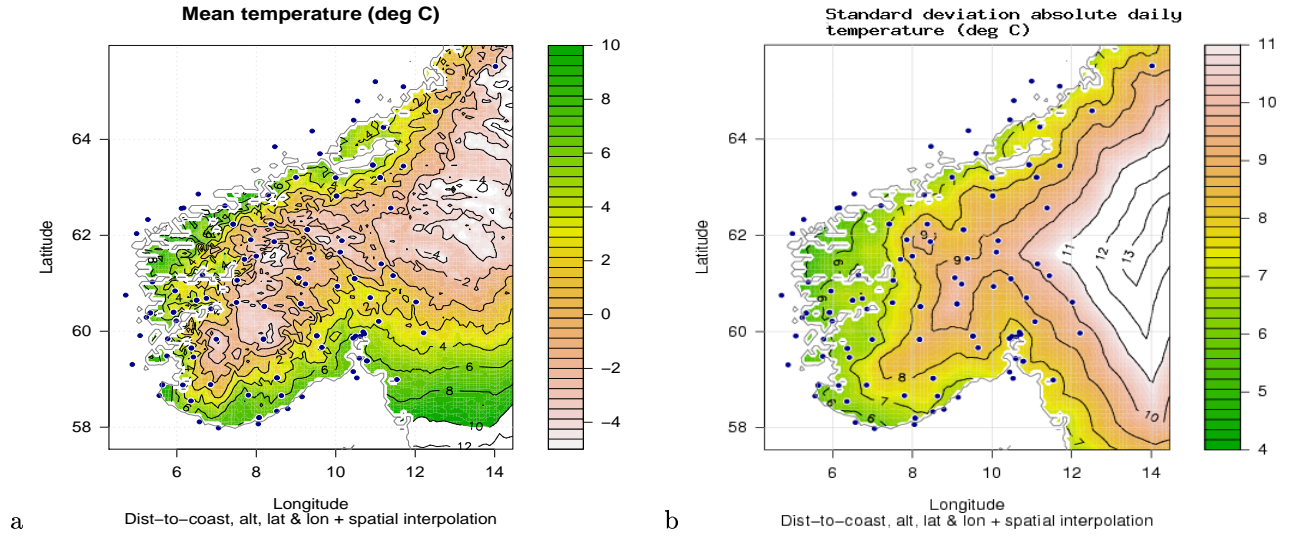


Figure 3. The spatial interpolation of the mean temperature (a) and temperature variability (b) using a multiple regression model (Table 1) against the geographical parameters distance from the coast, altitude, latitude, longitude, north-south slope, and the east-west slope.

TABLE 1. Summary of the multiple regression of mean temperature (upper) and standard deviation of the temperature (lower) against distance from the coast, altitude, latitude, longitude, north-south slope and east-west slope. [**Mean**: Residual standard error: 0.9137 on 74 degrees of freedom Multiple R-Squared: 0.8801, Adjusted R-squared: 0.8703 F-statistic: 90.5 on 6 and 74 DF, p-value: < 2.2e-16; **Std**: Residual standard error: 0.7994 on 74 degrees of freedom Multiple R-Squared: 0.7293, Adjusted R-squared: 0.7073 F-statistic: 33.22 on 6 and 74 DF, p-value: < 2.2e-16]

Mean(T2m)	Estimate	Std. Error	t value	Pr(> t)
(Intercept)	22.3347	4.8007	4.65	0.0000
dist	-1.4236	0.3170	-4.49	0.0000
alt	-0.0056	0.0004	-14.67	0.0000
lat	-0.2325	0.0822	-2.83	0.0060
lon	-0.1675	0.0565	-2.96	0.0041
grad.ns	-0.0000	0.0001	-0.20	0.8400
grad.ew	-0.0000	0.0001	-0.19	0.8466
Std(T2m)	Estimate	Std. Error	t value	Pr(> t)
(Intercept)	19.5512	4.2000	4.66	0.0000
dist	1.7505	0.2773	6.31	0.0000
alt	0.0001	0.0003	0.36	0.7235
lat	-0.2713	0.0719	-3.77	0.0003
lon	0.4019	0.0494	8.13	0.0000
grad.ns	-0.0001	0.0001	-1.79	0.0778
grad.ew	0.0001	0.0001	0.85	0.3971

interpolation of the mean temperature and amplitude (standard deviation) according to this multiple regressional geographic model. The multiple regression is summarized in Table 1: the mean temperature is strongly depending on the distance from the coast, altitude, latitude and longitude. The slope aspects are less important for the mean temperature. The entire multiple regression accounts for 88% of the spatial variance in the mean temperature (Table 1, upper), hence there is a strong association between the mean temperature and geographical parameters, justifying the use of similar geographical modeling for the spatial interpolation of the downscaled warming estimates. Likewise, the distance from the coast, longitude and latitude are important parameters for the temperature amplitude, whereas the altitude, and slope aspects are less important. The multiple linear regression model accounts for 73% of the spatial distribution in the temperature variance, also indicating a close dependence on geographical parameters. It is important to keep in mind that the various geographical parameters used here are not orthogonal (i.e. the result may be sensitive to the order of the geographical parameters in the multiple regression).

For the downscaling, the geographical model used different weights ($R_i^2 / \sum_i R_i^2$) where $i = 1 \dots N$

TABLE 2. A comparison of the spread in temperature change estimates from the HIRHAM RCM and from further empirical downscaling.

	min	max	median	mean	$R^2 >$
Winter					
RCM:	0.8281	1.2250	1.0610	1.0620	
DS:	-0.5535	1.6770	0.9910	0.8729	0%
DS:	0.5482	1.6770	1.0110	1.0130	30%
DS:	0.5482	1.6770	1.0120	1.0240	40%
DS:	0.5482	1.6770	1.0110	1.0170	50%
DS:	0.5482	1.6770	1.0060	1.0130	60%
DS:	0.5482	1.6770	1.0150	1.0200	70%
DS:	0.7311	1.6770	1.0150	1.0520	75%
Spring					
RCM:	0.6013	0.9264	0.8159	0.8024	
DS:	-0.1438	1.5560	0.9279	0.8204	0%
DS:	0.5595	1.1320	1.0160	1.0010	30%
DS:	0.7429	1.1320	1.0170	1.0090	40%
DS:	0.7429	1.1320	1.0190	1.0130	50%
DS:	0.7429	1.1320	1.0190	1.0200	60%
DS:	0.8482	1.1320	1.0940	1.1050	70%
DS:	0.889	1.1320	1.170	1.175	75%
Summer					
RCM:	0.878	1.515	1.272	1.244	
DS:	-0.3053	1.1010	0.8155	0.7104	0%
DS:	0.4770	0.9205	0.8480	0.8402	30%
DS:	0.4770	0.9205	0.8577	0.8494	40%
DS:	0.4770	0.9205	0.8658	0.8593	50%
DS:	0.4770	0.9205	0.8790	0.8613	60%
DS:	0.5791	0.9205	0.8658	0.8662	70%
DS:	0.5791	0.9205	0.8794	0.8718	75%
Autumn					
RCM:	0.8216	1.4330	1.2250	1.2040	
DS:	-0.3362	1.4700	0.8483	0.7383	0%
DS:	0.5626	1.0380	0.8985	0.8953	30%
DS:	0.5821	1.0430	0.9151	0.9054	40%
DS:	0.5821	1.0440	0.9154	0.9056	50%
DS:	0.5821	1.0700	0.9157	0.9124	60%
DS:	0.9936	1.0480	1.0250	1.0300	70%
DS:	0.9936	0.9936	0.9936	0.9936	75%

for the N different stations in order to take into account the differences in the skill of the different downscaling models. The residual from the geographical model was spatially interpolated using a bilinear interpolation scheme (using the R package *akima*).

3 Results

The range of temperature change estimated for the different locations was examined both from the RCM results and the further empirical downscaling analysis. In general, the empirical downscaling increases the range of the estimates. For some locations, the empirical suggest a cooling for the future, but these negative estimates are associated with low R^2 and low downscaling model skill. Table 2 shows the spread of estimates for the subsets of stations with downscaling skill-scores exceeding a set of threshold values $R^2 > [0\%, 30\%, 40\%, 50\%, 60\%, 70\%, 75\%]$. For stations with $R^2 > 30\%$, the range is relatively robust, and all estimates are greater than zero and the lowest value for $\Delta T(2m)$ is 0.55°C , the maximum value is 1.67°C , the median 1.01°C and mean = 1.01°C .

3.1 Winter: December – February

TABLE 3. A summary of the downscaled scenarios for the different stations. The columns list the longitude ($^{\circ}\text{E}$), latitude ($^{\circ}\text{N}$), altitude (m. a.s.l), the variance accounted for by the multiple regression (%), estimated temperature change ($^{\circ}\text{C}$), corresponding t-test, the proportional change in variance between the scenario and the control intervals, and the estimated change in the 95 and 5 percentiles ($^{\circ}\text{C}$).

	location	station no.	lon	lat	alt	R^2	p-value	ΔT	t-test	δ var	q95	q05
1	Røros	10400	11.38	62.57	628	75	0	0.67	0	0.89	0.33	1.56
2	Prestebakke	1130	11.54	58.99	157	31	0	0.86	0	0.92	0.72	1.16
3	Østre	11500	10.87	60.70	264	72	0	0.65	0	0.96	0.94	1.19
4	Lillehammer	12680	10.48	61.09	114	72	0	0.76	0	0.92	0.94	1.55
5	Venabu	13420	10.11	61.65	930	72	0	0.78	0	0.94	0.74	1.01
6	Skåbu	13670	9.38	61.52	890	62	0	0.90	0	0.94	0.89	1.19
7	Gjeilo	15540	8.45	61.87	378	73	0	0.79	0	0.91	0.84	1.85
8	Bråtå	15720	7.86	61.91	712	75	0	0.86	0	0.92	0.78	1.35
9	Fokstua	16610	9.29	62.11	386	78	0	1.14	0	0.95	1.19	1.49
10	Rygge	17150	10.79	59.38	205	75	0	1.39	0	0.94	1.38	2.17
11	Jeløy	17290	10.59	59.44	12	77	0	0.99	0	0.95	1.08	1.42
12	Oslo	18700	10.72	59.94	380	76	0	1.01	0	0.96	1.09	1.36
13	Tryvasshøgda	18960	10.69	59.99	528	75	0	0.93	0	0.92	0.77	1.30
14	Fornebu	19400	10.62	59.89	10	74	0	1.01	0	0.95	1.12	1.46
15	Dønski	19480	10.50	59.90	59	71	0	0.87	0	0.98	1.11	1.35
16	Asker	19710	10.44	59.86	163	3	0	-0.55	0	0.98	-0.71	-0.51
17	Vest-torpa	21680	10.04	60.94	542	75	0	0.55	0	0.93	0.76	1.12
18	Fagernes	23420	9.24	60.99	365	71	0	1.03	0	0.90	0.87	2.13
19	Løken	23500	9.07	61.12	525	71	0	0.60	0	0.96	0.95	1.17
20	Nesbyen	24880	9.12	60.57	70	71	0	1.07	0	0.91	1	2.14
21	Geilo	25590	8.20	60.52	353	76	0	1.10	0	0.94	1.17	1.43
22	Finse	25840	7.50	60.60	1224	11	0	0.49	0	0.99	0.54	0.59
23	Måkerøy	27410	10.44	59.16	43	49	0	0.87	0	0.94	0.89	1.34
24	Færder	27500	10.53	59.03	6	77	0	1.02	0	0.92	0.97	1.56
25	Kongsberg	28370	9.65	59.66	168	74	0	0.96	0	0.94	1.11	1.66
26	Lungdal	28800	9.52	59.91	142	75	0	1.06	0	0.93	1.14	1.87
27	Magnor	2950	12.21	59.97	154	75	0	1.41	0	0.94	1.54	1.84
28	Møsstrand	31620	8.18	59.84	388	13	0	0.47	0	0.97	0.58	0.60
29	Lyngør	35860	9.15	58.63	4	77	0	1.02	0	0.92	0.84	1.58
30	Torungen	36200	8.79	58.38	12	77	0	1	0	0.92	0.86	1.61
31	Nelaug	36560	8.63	58.66	142	57	0	1.21	0	0.96	1.12	1.87
32	Tveitsund	37230	8.52	59.03	124	75	0	1.32	0	0.93	1.26	2.07
33	Landvik	38140	8.52	58.33	6	67	0	0.92	0	0.99	1.10	1.31
34	Kjevik	39040	8.07	58.20	23	74	0	1.22	0	0.94	1.16	1.93
35	Oksøy	39100	8.05	58.07	9	77	0	1	0	0.93	0.81	1.57
36	Byglandsfjord	39690	7.80	58.67	212	73	0	1.12	0	0.93	1.05	1.73
37	Lindesnes	41770	7.05	57.98	13	77	0	0.93	0	0.93	0.79	1.48
38	Lista	42160	6.57	58.11	14	77	0	0.96	0	0.93	0.86	1.59
39	Sirdal	42920	6.85	58.89	242	9	0	0.26	0	0.99	0.36	0.39
40	Ualand	43500	6.35	58.55	196	73	0	1.04	0	0.96	1.06	1.66
41	Obrestad	44080	5.56	58.66	24	76	0	1.01	0	0.95	1.03	1.51
42	Sola	44560	5.64	58.88	312	75	0	1.02	0	0.94	1.08	1.53
43	Suldal	46200	6.42	59.46	58	68	0	1.24	0	0.93	1.16	1.80
44	Midtlæger	46510	6.99	59.83	1079	31	0	0.56	0	1.03	0.78	0.75
45	Sauda	46610	6.36	59.65	240	72	0	1.06	0	0.92	0.98	1.75
46	Nedre	46910	5.75	59.48	64	74	0	1.15	0	0.95	1.25	1.55
47	Utsira	47300	4.88	59.31	55	78	0	0.75	0	0.94	0.78	1.11
48	Gardermoen	4780	11.08	60.21	202	76	0	1.12	0	0.96	1.26	1.66
49	Slåttery	48330	5.07	59.91	15	77	0	0.73	0	0.95	0.74	1.10

TABLE 3. Table continued...

	location	station no.	lon	lat	alt	R^2	p-value	ΔT	t-test	δ var	q95	q05
50	Upsangervatn	48390	5.77	59.84	60	3	0	0.15	0	0.80	0.06	0.23
51	Eidfjord	49580	6.86	60.47	165	8	0	0.03	0.17	0.99	0.02	0.11
52	Omastrand	50130	5.98	60.22	2	75	0	0.87	0	0.95	0.85	1.27
53	Kvamskogen	50300	5.91	60.39	210	76	0	1.12	0	0.96	1.28	1.63
54	Flesland	50500	5.23	60.29	48	79	0	1.03	0	0.95	1.17	1.45
55	Bergen	50540	5.33	60.38	23	77	0	1	0	0.95	1.14	1.43
56	Voss	51590	6.50	60.65	30	76	0	1.39	0	0.93	1.47	2.41
57	Reimegrend	51670	6.74	60.69	590	55	0	1.01	0	0.95	1.17	1.59
58	Modalen	52290	5.95	60.84	114	74	0	1.23	0	0.94	1.14	1.77
59	Hellisøy	52530	4.71	60.75	20	1	1	0.08	0	1.30	0.11	0.03
60	Takle	52860	5.38	61.03	38	80	0	0.98	0	0.95	1.11	1.36
61	Vangnes	53100	6.65	61.17	51	65	0	0.64	0	0.96	0.70	0.84
62	Lærdal	54130	7.52	61.06	36	74	0	0.95	0	0.93	0.91	1.57
63	Fortun	55160	7.70	61.50	27	77	0	1.07	0	0.93	1.01	1.76
64	Sognefjell	55290	8	61.57	1413	80	0	1.22	0	0.99	1.39	1.47
65	Kråkenes	59100	4.99	62.03	41	7	0	0.27	0	0.72	0.16	0.37
66	Svinøy	59800	5.27	62.33	38	79	0	0.82	0	0.96	0.87	0.96
67	Flisa	6040	12.02	60.61	184	49	0	1.41	0	0.93	1.42	2.10
68	Tafjord	60500	7.42	62.23	52	13	0	0.34	0	1	0.33	0.42
69	Vigra	60990	6.12	62.56	106	79	0	0.95	0	0.95	1.01	1.20
70	Hjelvik	61170	7.21	62.62	21	80	0	0.97	0	0.94	0.95	1.28
71	Lesjaskog	61770	8.37	62.23	621	75	0	1.17	0	0.94	1.31	1.95
72	Ona	62480	6.54	62.86	13	2	0	0.16	0	0.94	0.17	0.17
73	Tingvoll	64550	8.30	62.84	69	73	0	0.84	0	0.91	0.87	1.23
74	Vinjøera	65110	9	63.21	229	5	0	0.25	0	0.90	0.24	0.33
75	Sula	65940	8.47	63.85	5	52	0	0.69	0	0.94	0.65	0.82
76	Berkaak	66730	10.02	62.82	231	76	0	0.95	0	0.93	0.88	1.40
77	Selbu	68340	11.12	63.21	117	14	0	0.50	0	0.99	0.53	0.62
78	Vaernes	69100	10.94	63.46	23	78	0	1.07	0	0.88	0.74	1.49
79	Meråker	69330	11.70	63.44	145	76	0	1.12	0	0.88	0.65	1.67
80	Rena	7010	11.44	61.16	240	74	0	1.32	0	0.95	1.44	2.55
81	Ørland	71550	9.60	63.70	10	79	0	0.96	0	0.90	0.72	1.36
82	Halten	71850	9.41	64.17	16	78	0	0.90	0	0.92	0.81	1.10
83	Buholmråsa	71990	10.45	64.40	18	81	0	1.13	0	0.91	1.04	1.34
84	Namdalseid	72100	11.20	64.25	86	1	3	-0.04	0	1.01	-0.01	-0.04
85	Harran	73620	12.51	64.59	118	75	0	1.35	0	0.86	0.92	2
86	Nordøyen	75410	10.55	64.80	33	7	0	-0.37	0	1.14	-0.40	-0.50
87	Sklinna	75550	11	65.20	23	83	0	1.05	0	0.90	1.10	1.31
88	Leka	75600	11.70	65.10	47	32	0	1.04	0	0.90	0.89	1.37
89	Susendal	77750	14.02	65.52	265	76	0	1.68	0	0.88	1.60	2.54
90	Evenstad	8130	11.14	61.41	255	25	0	0.31	0	1.11	0.64	0.44
91	Sørneset	8710	10.15	61.89	739	11	0	0.25	0	0.93	0.22	0.33

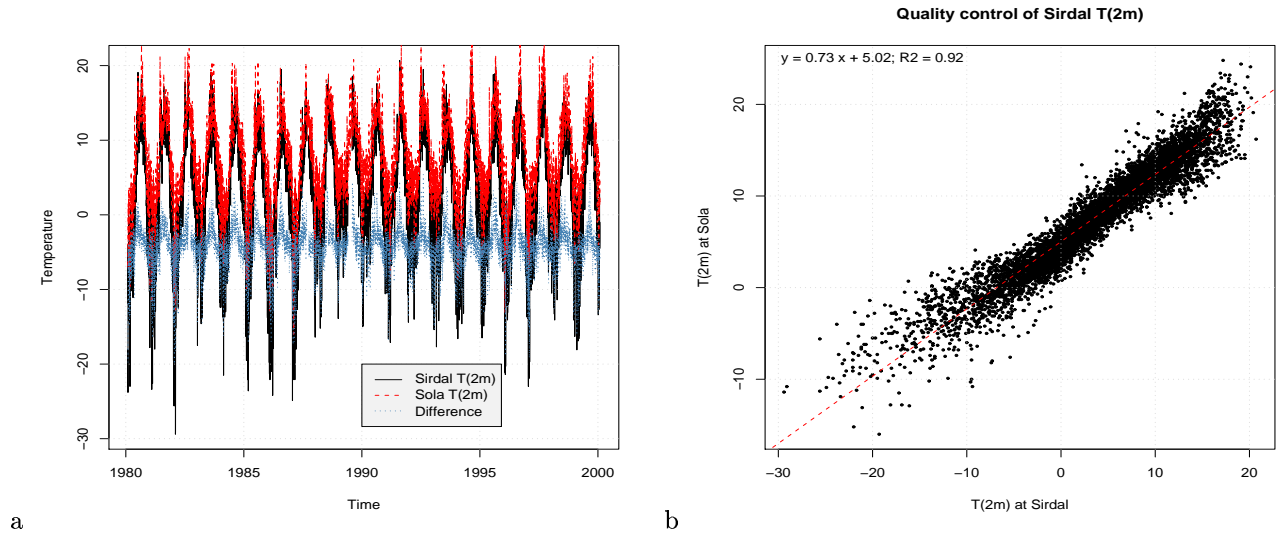


Figure 4. Quality test of the daily temperature at Sirdal. Panel (a) shows the time series at Sirdal and Sola, (b) a scatter plot and best-linear-fit.

TABLE 4. A comparison between the multiple regression models used in the empirical downscaling at Sirdal and Sola.

Statistical significance codes are: 0 '***' 0.1 '**' 0.01 '*' 0.05 '.' 0.1 ' ' 1.

PC	Estimate	Std. Error	t value	Pr(> t)
Sirdal				
(Intercept)	-9.804×10^{17}	1.372×10^{01}	-7.15×10^{16}	1 00
X1	-4.347×10^{02}	7.207×10^{03}	-6.033	2.12×10^{09} ***
X2	-1.023×10^{01}	1.812×10^{02}	-5.647	2.02×10^{08} ***
X3	1.737×10^{01}	2.394×10^{02}	7.254	7.03×10^{13} ***
X4	-6.108×10^{02}	4.052×10^{02}	-1.508	0.1319
X5	-8.1×10^{02}	4.010×10^{02}	-1.995	0.0463 *
X8	-1.542×10^{01}	6.493×10^{02}	-2.374	0.0177 *
Sola				
(Intercept)	-2.401×10^{17}	5.776×10^{02}	-4.16×10^{16}	1
X1	-1.237×10^{01}	3.145×10^{03}	-39.330	$< 2 \times 10^{16}$ ***
X2	-2.262×10^{01}	7.711×10^{03}	-29.332	$< 2 \times 10^{16}$ ***
X3	2.072×10^{01}	1.031×10^{02}	20.102	$< 2 \times 10^{16}$ ***
X4	-1.900×10^{01}	1.796×10^{02}	-10.575	$< 2 \times 10^{16}$ ***
X5	-2.064×10^{01}	1.710×10^{02}	-12.067	$< 2 \times 10^{16}$ ***
X6	2.916×10^{01}	1.852×10^{02}	15.747	$< 2 \times 10^{16}$ ***
X7	2.474×10^{01}	3.113×10^{02}	7.948	4.21×10^{15} ***
X8	-2.669×10^{01}	3.044×10^{02}	-8.766	$< 2 \times 10^{16}$ ***

Table 3 (column 6) gives an indication of how much of the December–February temperature variance that the empirical downscaling can reproduce. In most locations, the empirical downscaling can reproduce more than 70% of the local variance during the winter season, but the ANOVA results also suggest that the empirical downscaling model was poor for some locations (Prestebakke, Asker, Finse, Måkerøy, Møsstrand, Sirdal, Midtlæger, Upsangervatn, Eidfjord, Hellisøy, Kråkenes, Flisa, Tafjord, Ona, Vinjeøra, Selbu, , Namdalseid, Nordøyen, Lekå, Evenstad, and Sørnesset). Low R^2 -values may indicate low data quality or a weak relationship between large-scale features and local temperature.

In order to examine whether the temperatures at those stations with low values for R^2 were due to data degradation, the Sirdal temperatures were compared with temperatures at the nearby station Sola which achieved $R^2 = 0.75$ (Figure 4). It is interesting to note the good agreement between the temperature at Sola and Sirdal ($R^2 = 0.92$), and the difference between the two data records (blue curve in Figure 4) does not give any clear indication of spurious data. The greatest differences were, however, found during the coldest days. The situation of the two stations is characterised by a 493m-height difference, Sola being near the sea level (7m a.s.l). A closer look at the downscaling results indicates that the regression model fails to describe the local variations (Figure 5(a)–(b)), and trials with different

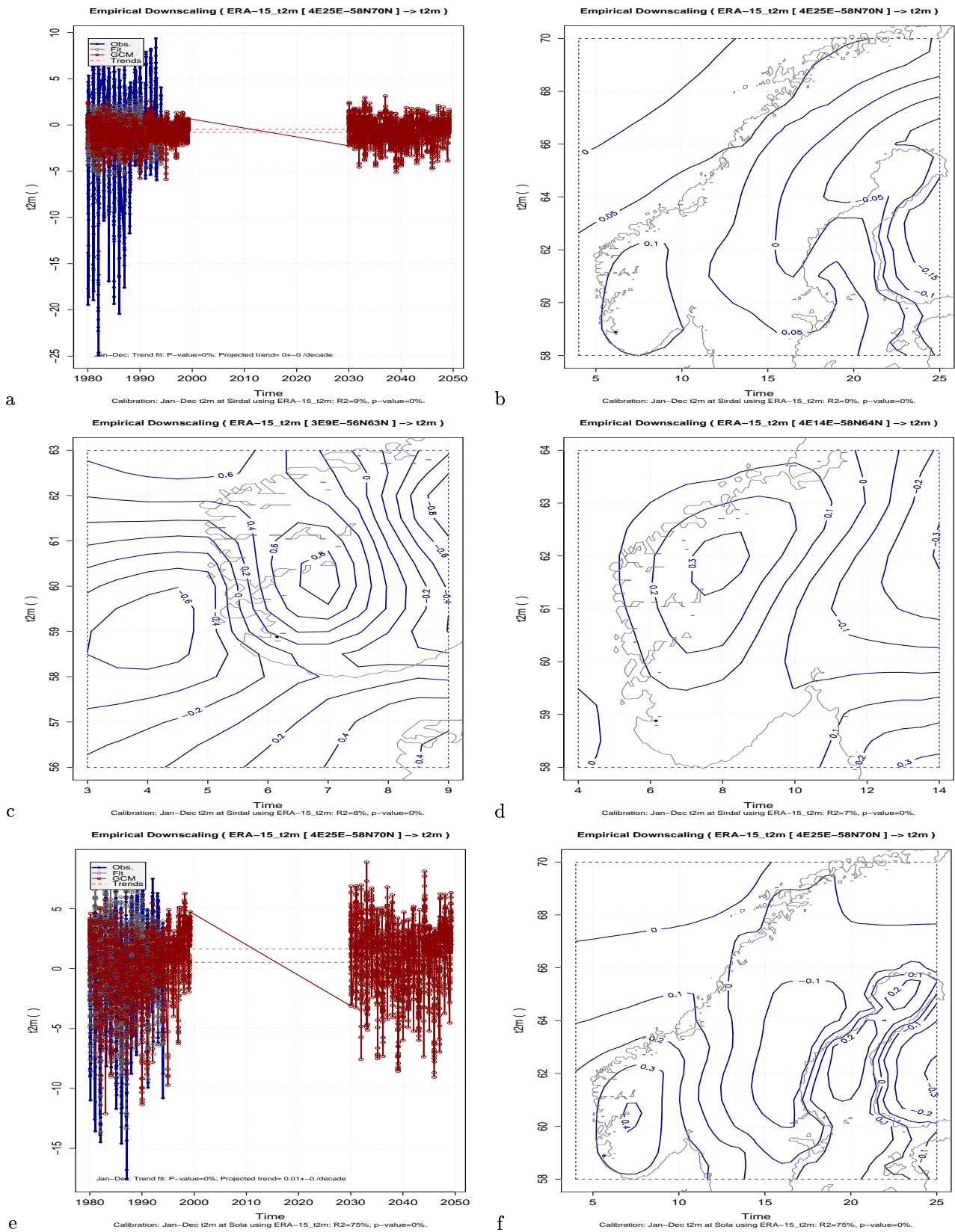


Figure 5. (a) The time series from the downscaling, and (b)–(d) the spatial pattern of the combined ERA-15/ECHAM4 temperature field related to the station values at Sirdal (regression against ERA-15 values only) for different predictor domains. Panels (e)–(f) show the downscaled results for Sola.

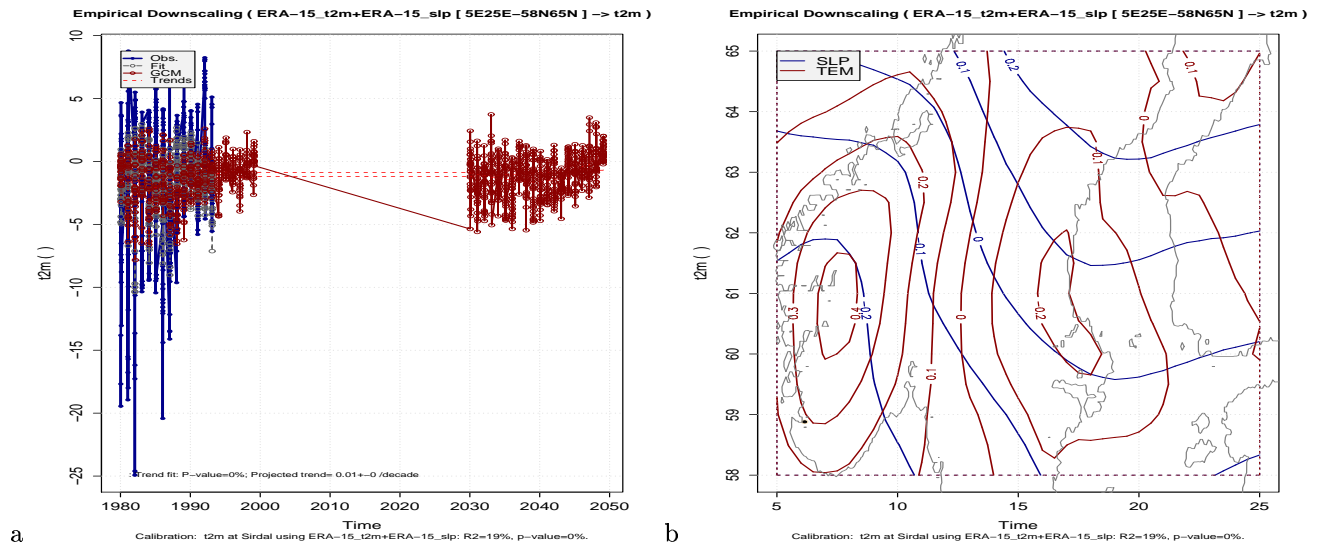


Figure 6. The same as Figure 5, but using mixed-common T(2m)-SLP EOFs (*Benestad et al., 2002*) and the R 'glm' model.

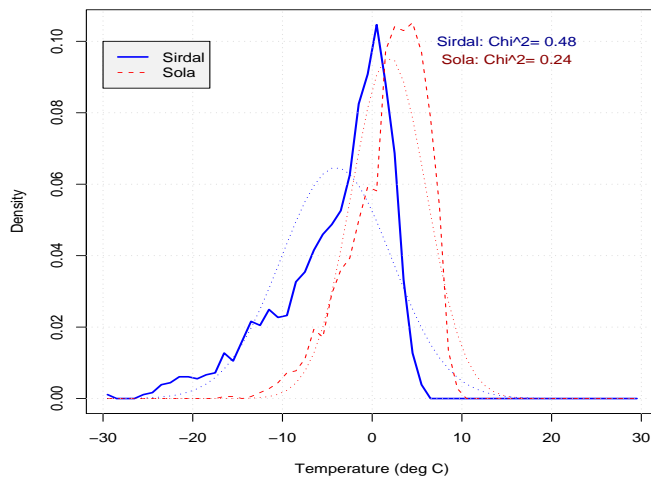


Figure 7. A comparison between the histograms of the December–February temperature at Sirdal and Sola reveals a stronger degree of non-normality at Sirdal. The best-fit Gaussian distributions are also shown as dotted lines.

spatial domains give the same poor results (Figure 5(c)–(d)). A comparison with the downscaled results for Sola (Figure 5(e)–(f)) suggests that the multiple model does not capture the small scale features sufficiently well. The empirical model differences are summarized in Table 4. It is apparent that the EOF-modes of orders 5–8, describing the smaller scales, are weakly related to the temperature in Sirdal but strongly related to the temperature at Sola. The close association between the temperatures at Sola and Sirdal, apparent from Figure 4, may suggest that the relationship with the ERA-15 temperature field may be corrupted by small errors or that the temperature in Sirdal is strongly affected by regional (also affecting Sola) and local conditions. Figure 6 shows the downscaling analysis repeated on mixed T(2m)-SLP predictor fields and using a general linear model, and the R^2 -value is now 19%. Studies with analog models, also suggest that the temperature can be reproduced with a correlation of 0.56, rmse 4.89°C (*Alexandra Imbert, private communications*). The failure to reproduce the local temperature with linear models may be a result of the Sirdal temperature having a more non-Gaussian distribution (Figure 7). A χ^2 -test (*Wilks, 1995, p. 133*) gives higher values for Sirdal than for Sola, indicating a worse

TABLE 5. A summary of the multiple regression according to equation (1) for the downscaled winter (December–February) results. [Residual standard error: 0.02193 on 74 degrees of freedom Multiple R-Squared: 0.1587, Adjusted R-squared: 0.09051 F-statistic: 2.327 on 6 and 74 DF, p-value: 0.04106].

	Estimate	Std. Error	t value	Pr(> t)
(Intercept)	1.38853705	1.21142481	1.15	0.26
dist	-0.03530103	0.08860718	-0.40	0.69
alt	-0.00009271	0.00011522	-0.80	0.42
lat	-0.01173944	0.02082898	-0.56	0.58
lon	0.04285448	0.01543990	2.78	0.01
grad.ns	0.00001000	0.00002261	0.44	0.66
grad.ew	0.00005419	0.00002289	2.37	0.02

fit for Sirdal. It is also possible that the relationship between the Sola temperature and the synoptic temperature pattern is more linear than for Sirdal.

The empirical downscaled results indicate warming for most of the locations, with lowest value for $\Delta T(2m)$ of -0.55°C and maximum value of 1.67°C , a median of 0.99°C and mean = 0.87°C (Table 2). Only three stations gave negative values, and these were associated with low downscaling skill-scores (Asker: $R^2 = 3\%$ and $\Delta T = -0.55$; Namdalseid: $R^2 = 1\%$ and $\Delta T = -0.04$; Nordøyen: $R^2 = 7\%$ and $\Delta T = -0.37$). In comparison, the corresponding values from the HIRHAM temperatures are: 0.83°C 1.23°C 1.06°C and 1.06°C respectively. In other words, the refined temperatures suggest a greater geographical spread than HIRHAM with a range that extends both below and above the lowest and highest HIRHAM values respectively. In contrast, *Skaugen et al. (2002)* obtained systematically weaker warming as a result of a reduction in the variance. The variance reported by *Skaugen et al. (2002)* have similar magnitudes as those listed in Table 3, so the higher values obtained by the present empirical downscaling is related to differences in the large-scale temperature patterns in the ERA-15 data and the RCM results.

Table 3 contains information about changes in the temperature ranges in terms of the proportional change in the variance ($\text{var}(T_{\text{sce}})/\text{var}(T_{\text{ctl}})$) and changes in the 95 and 5 percentiles. The downscaled winter temperature scenarios suggest a general reduction in the min–max temperature range, with the lowest temperatures (5 percentile) increasing faster than the high temperatures (95 percentile). However, there are some exceptions concerning a number of stations associated with low downscaling skill-scores: Midtlæger ($R^2 = 0.31$) $\delta \text{ var} = 1.03$; Hellsøy ($R^2 = 0.01$) $\delta \text{ var} = 1.30$; Tafjord ($R^2 = 0.13$) $\delta \text{ var} = 1.00$; Namdalseid ($R^2 = 0.01$) $\delta \text{ var} = 1.01$; Nordøyen ($R^2 = 0.07$) $\delta \text{ var} = 1.14$; Evenstad ($R^2 = 0.25$) $\delta \text{ var} = 1.11$.

The spatial interpolation employed the statistical geographical model described by equation (1) and the model is summarized in Table 5. The geographical model describes about 16% of the spatial variance in the change estimates for the winter season, the F-statistic = 2.327, and p-value = 0.04. However, the p-values associated with the individual geographical parameters suggest that only the dependence to longitude and the east–west gradient are statistically significant at the 5% level. Hence, the longitude and east–west slope are the two most important geographical parameters during winter, however the effect of the altitude, latitude, north–south slope and the distance from the coast may also play a small role. An interpolation produced by the geographical model is shown in Figure 8b, and Figure 8c shows a map of the regression residuals (the error $\eta = y - \hat{y}$ using equation (1)) derived using a bi-linear spatial interpolation.

The refined scenario (Figure 8d) consists of the sum of the geographical model (Figure 8b) and the spatial interpolation of the residuals (Figure 8c). This scenario suggests temperature change in winter of similar magnitude as the HIRHAM scenario (Figure 8e), but local geographical features are more prominent in the results based on the empirical downscaling analysis. The refined scenario indicates a slightly weaker warming than the original HIRHAM scenario over most of southern Norway except for over Østfold (Figure 8f). It is interesting to note correlation between the weaker warming estimates and low downscaling skill-score (the correlation between ΔT and R^2 is 0.86).

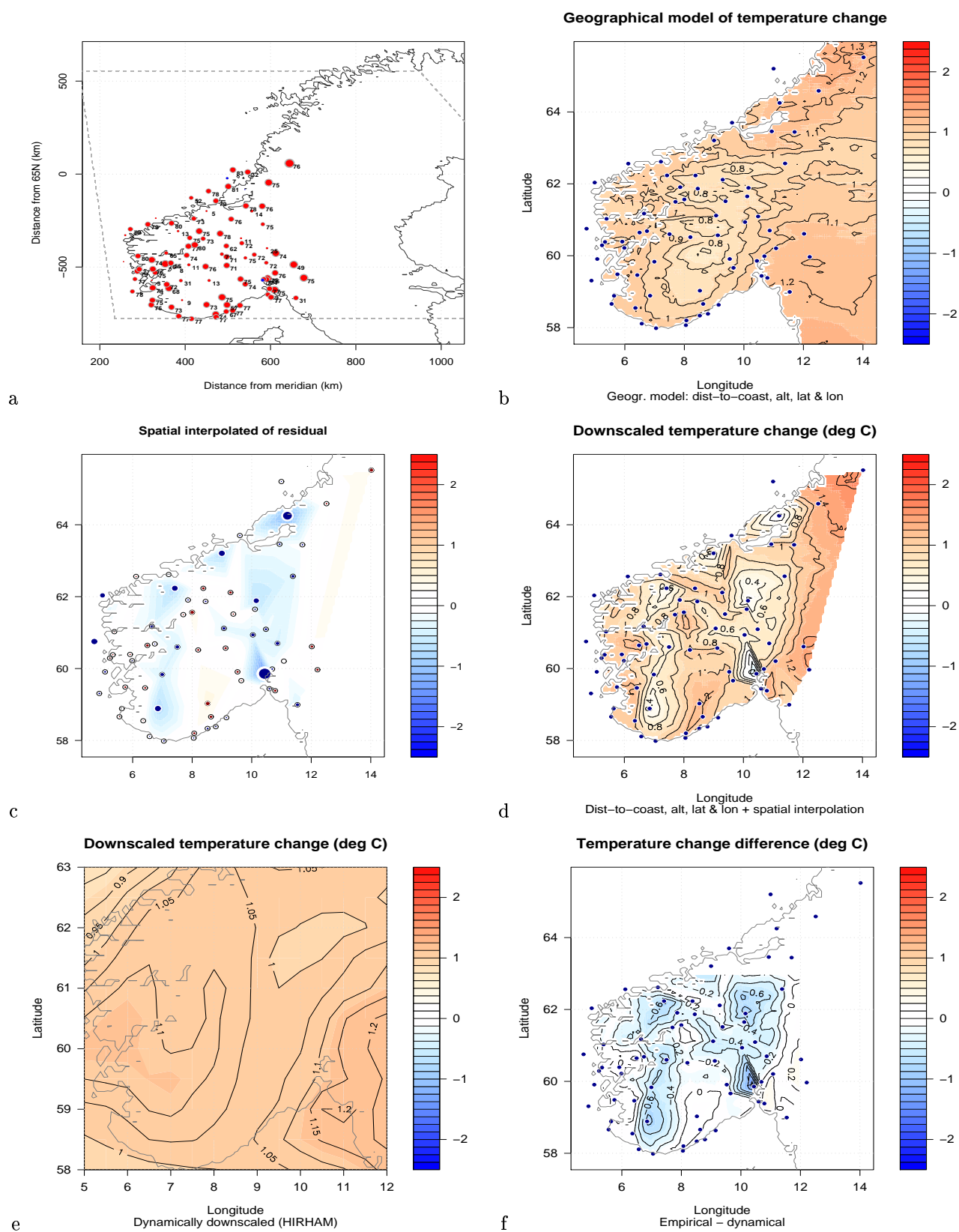


Figure 8. (a) the refined scenario, (b) the HIRHAM scenario, (c) refined - HIRHAM, (d) map of locations for empirical downscaling indicating the magnitude of change, (e) results from the geographical model, and (f) the spatial interpolation of the residual from the geographical model.

3.2 Spring: March – May

The downscaled results for the spring season are shown in Figure 9 and the statistics is summarized in Tables 6–6. The regression variance in Table 6 (R^2) indicates that the stations with low R^2 values were the same as in winter (Table 3) and spring, but there were also some additional locations with low scores ($R^2 < 0.50$) for the spring-time downscaling (Reimegrend, Nelaug, Sula). The R^2 for the “good stations” were in the range 51–83%. The estimated temperature change is on average slightly lower in spring than in winter (Table 2). The variance accounted for by the geographical model (equation (1)) was 57%, and the downscaled warming exhibited a clear and statistically significant dependency to the latitude and longitude (Table 6). The north–south slope and distance from the coast may also play a role for the projected warming. A comparison between the refined values and the output from the RCM suggests that the empirical downscaling produces slightly stronger spring time warming in the east and weaker warming in the west. There is a general tendency suggesting a future reduction in the daily mean

TABLE 6. Same as Table 3, but for the spring season (March–May).

location	station no.	lon	lat	alt	R^2	p-value	ΔT	t-test	δ var	q95	q05
1 Røros	10400	11.38	62.57	628	76	0	1.34	0	0.84	0.53	1.56
2 Prestebakke	1130	11.54	58.99	157	9	0	0.44	0	0.74	0.21	0.76
3 Østre	11500	10.87	60.70	264	57	0	1.06	0	0.77	0.08	1.39
4 Lillehammer	12680	10.48	61.09	114	72	0	1.09	0	0.77	0.13	1.55
5 Venabu	13420	10.11	61.65	930	76	0	1.17	0	0.84	0.33	1.38
6 Skåbu	13670	9.38	61.52	890	52	0	0.93	0	0.81	0.20	1.27
7 Gjeilo	15540	8.45	61.87	378	61	0	1.15	0	0.80	0.16	1.38
8 Bråtå	15720	7.86	61.91	712	76	0	1.17	0	0.85	0.45	1.34
9 Fokstua	16610	9.29	62.11	386	80	0	1.21	0	0.89	0.66	1.23
10 Rygge	17150	10.79	59.38	205	73	0	1.02	0	0.72	0.09	1.52
11 Jeløy	17290	10.59	59.44	12	63	0	0.88	0	0.68	-0.02	1.47
12 Oslo	18700	10.72	59.94	380	69	0	0.95	0	0.76	0.23	1.33
13 Tryvasshøgda	18960	10.69	59.99	528	60	0	1.03	0	0.77	0.20	1.43
14 Fornebu	19400	10.62	59.89	10	66	0	1.02	0	0.71	0.04	1.60
15 Dønski	19480	10.50	59.90	59	65	0	0.97	0	0.73	0.07	1.46
16 Asker	19710	10.44	59.86	163	5	0	-0.06	0	0.92	-0.09	-0.01
17 Vest–torpa	21680	10.04	60.94	542	76	0	1.02	0	0.81	0.21	1.30
18 Fagernes	23420	9.24	60.99	365	70	0	1.04	0	0.75	0.07	1.31
19 Løken	23500	9.07	61.12	525	59	0	0.97	0	0.79	0.02	1.15
20 Nesbyen	24880	9.12	60.57	70	67	0	1.08	0	0.73	-0.02	1.43
21 Geilo	25590	8.20	60.52	353	73	0	1.13	0	0.78	0.07	1.42
22 Finse	25840	7.50	60.60	1224	5	0	0.32	0	0.75	0.01	0.45
23 Måkerøy	27410	10.44	59.16	43	43	0	0.50	0	0.73	0.08	0.73
24 Færder	27500	10.53	59.03	6	69	0	0.86	0	0.67	-0.06	1.50
25 Kongsberg	28370	9.65	59.66	168	66	0	1.07	0	0.71	0.09	1.55
26 Lungdal	28800	9.52	59.91	142	71	0	1.04	0	0.74	0.06	1.44
27 Magnor	2950	12.21	59.97	154	72	0	1.15	0	0.73	0.14	1.68
28 Møsstrand	31620	8.18	59.84	388	5	0	0.22	0	0.68	-0.06	0.42
29 Lyngør	35860	9.15	58.63	4	62	0	0.82	0	0.67	-0.03	1.47
30 Torungen	36200	8.79	58.38	12	63	0	0.78	0	0.66	-0.08	1.38
31 Nelaug	36560	8.63	58.66	142	43	0	0.82	0	0.66	-0.12	1.28
32 Tveitsund	37230	8.52	59.03	124	69	0	1.01	0	0.69	-0.03	1.54
33 Landvik	38140	8.52	58.33	6	51	0	0.75	0	0.70	-0.05	1.14
34 Kjevik	39040	8.07	58.20	23	68	0	0.83	0	0.71	0.03	1.24
35 Oksøy	39100	8.05	58.07	9	65	0	0.75	0	0.68	-0	1.33
36 Byglandsfjord	39690	7.80	58.67	212	66	0	0.97	0	0.70	-0.03	1.47
37 Lindesnes	41770	7.05	57.98	13	69	0	0.76	0	0.71	0.01	1.26
38 Lista	42160	6.57	58.11	14	68	0	0.80	0	0.75	0.09	1.21
39 Sirdal	42920	6.85	58.89	242	3	0	0.18	0	0.82	0.06	0.18
40 Ualand	43500	6.35	58.55	196	67	0	0.90	0	0.78	0.16	1.28
41 Obrestad	44080	5.56	58.66	24	67	0	0.82	0	0.74	0.06	1.22
42 Sola	44560	5.64	58.88	312	71	0	0.86	0	0.78	0.11	1.19
43 Suldal	46200	6.42	59.46	58	71	0	1.02	0	0.77	0.06	1.36
44 Midtlæger	46510	6.99	59.83	1079	13	0	0.30	0	1.01	0.30	0.38
45 Sauda	46610	6.36	59.65	240	68	0	0.81	0	0.81	0.11	1.03
46 Nedre	46910	5.75	59.48	64	72	0	0.97	0	0.81	0.22	1.17
47 Utsira	47300	4.88	59.31	55	66	0	0.74	0	0.74	0.01	0.98
48 Gardermoen	4780	11.08	60.21	202	67	0	1.13	0	0.72	0.15	1.65
49 Slåttery	48330	5.07	59.91	15	66	0	0.77	0	0.77	0.08	1

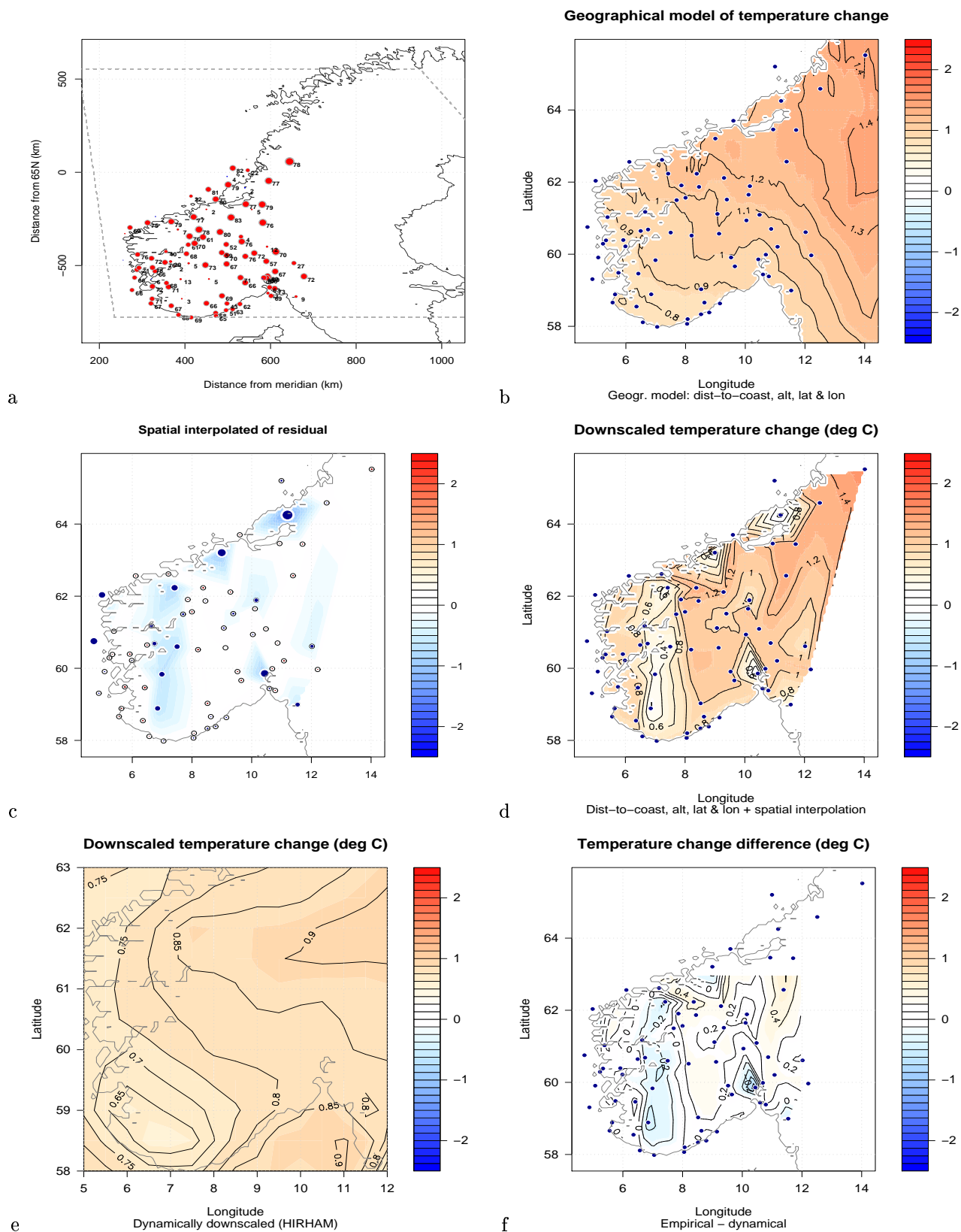


Figure 9. Same as in Figure 8, but for the spring season (March–May).

TABLE 5. Table continued...

	location	station no.	lon	lat	alt	R^2	p-value	ΔT	t-test	δ var	q95	q05
50	Upsangervatn	48390	5.77	59.84	60	6	0	-0.05	0	1.08	0.01	-0.04
51	Eidfjord	49580	6.86	60.47	165	2	0	0.08	0	0.82	0.02	0.13
52	Omastrand	50130	5.98	60.22	2	66	0	0.81	0	0.82	0.22	0.94
53	Kvamskogen	50300	5.91	60.39	210	78	0	0.95	0	0.83	0.23	1.09
54	Flesland	50500	5.23	60.29	48	71	0	0.88	0	0.81	0.15	1.03
55	Bergen	50540	5.33	60.38	23	71	0	0.85	0	0.83	0.24	0.98
56	Voss	51590	6.50	60.65	30	76	0	0.97	0	0.82	0.18	1.08
57	Reimegrend	51670	6.74	60.69	590	30	0	0.46	0	0.92	-0.03	0.40
58	Modalen	52290	5.95	60.84	114	72	0	0.93	0	0.81	0.14	1.06
59	Hellisøy	52530	4.71	60.75	20	2	0	-0.01	0.03	1.01	0.01	0.01
60	Takle	52860	5.38	61.03	38	76	0	0.89	0	0.83	0.22	0.98
61	Vangsnes	53100	6.65	61.17	51	40	0	0.56	0	0.84	0.05	0.63
62	Lærdal	54130	7.52	61.06	36	68	0	0.92	0	0.85	0.31	1.10
63	Fortun	55160	7.70	61.50	27	61	0	0.83	0	0.80	0.08	0.94
64	Sognefjell	55290	8	61.57	1413	70	0	1.14	0	0.87	0.36	1.31
65	Kråkenes	59100	4.99	62.03	41	2	0	0.10	0	1.17	0.12	0.04
66	Svinøy	59800	5.27	62.33	38	69	0	0.87	0	0.87	0.48	0.96
67	Flisa	6040	12.02	60.61	184	27	0	0.78	0	0.68	0.08	1.23
68	Tafjord	60500	7.42	62.23	52	7	0	0.32	0	0.89	0.36	0.43
69	Vigra	60990	6.12	62.56	106	75	0	1.02	0	0.88	0.53	1.13
70	Hjelvik	61170	7.21	62.62	21	79	0	1.12	0	0.90	0.61	1.20
71	Lesjaskog	61770	8.37	62.23	621	78	0	1.32	0	0.88	0.56	1.38
72	Ona	62480	6.54	62.86	13	2	0	-0.05	0	1.14	-0.02	-0.16
73	Tingvoll	64550	8.30	62.84	69	77	0	1.16	0	0.93	0.59	1.15
74	Vinjeøra	65110	9	63.21	229	2	0	0.18	0	0.81	0.10	0.30
75	Sula	65940	8.47	63.85	5	22	0	0.54	0	0.89	0.41	0.68
76	Berkaak	66730	10.02	62.82	231	83	0	1.30	0	0.91	0.81	1.28
77	Selbu	68340	11.12	63.21	117	5	0	0.21	0	0.97	0.42	0.29
78	Værnes	69100	10.94	63.46	23	77	0	1.24	0	0.92	0.98	1.37
79	Meråker	69330	11.70	63.44	145	79	0	1.33	0	0.91	0.98	1.48
80	Rena	7010	11.44	61.16	240	70	0	1.31	0	0.75	0.25	1.80
81	Ørland	71550	9.60	63.70	10	80	0	1.15	0	0.94	0.93	1.25
82	Halten	71850	9.41	64.17	16	81	0	0.95	0	0.92	0.65	1.07
83	Buholmråsa	71990	10.45	64.40	18	79	0	1.21	0	0.93	1.16	1.44
84	Namdalseid	72100	11.20	64.25	86	2	0	-0.14	0	1.05	-0.13	-0.37
85	Harran	73620	12.51	64.59	118	77	0	1.30	0	0.90	1.24	1.73
86	Nordøyen	75410	10.55	64.80	33	4	0	-0.09	0	0.88	-0.07	-0.01
87	Sklinna	75550	11	65.20	23	82	0	1.06	0	0.93	0.95	1.30
88	Leka	75600	11.70	65.10	47	22	0	0.67	0	0.94	0.81	0.88
89	Susendal	77750	14.02	65.52	265	78	0	1.56	0	0.90	1.62	1.99
90	Evenstad	8130	11.14	61.41	255	12	0	0.31	0	0.77	0.04	0.41
91	Sørneset	8710	10.15	61.89	739	4	0	0.73	0	0.74	0.05	1.05

TABLE 6. Same as Table 5, but for the spring season (March–May). [Residual standard error: 0.01342 on 74 degrees of freedom Multiple R-Squared: 0.5714, Adjusted R-squared: 0.5366 F-statistic: 16.44 on 6 and 74 DF, p-value: 6.14e-12].

	Estimate	Std. Error	t value	Pr(> t)
(Intercept)	-1.90008078	0.78791723	-2.41	0.02
dist	0.08759829	0.05935659	1.48	0.15
alt	0.00000329	0.00007911	0.04	0.97
lat	0.04293519	0.01359617	3.16	0.00
lon	0.02915444	0.01032568	2.82	0.01
grad.ns	-0.00002343	0.00001459	-1.61	0.11
grad.ew	-0.00000070	0.00001504	-0.05	0.96

temperature range*, and a stronger warming in the minimum daily temperatures[†] than in the maximum daily temperatures[‡].

*This range reflects the difference between the warmest and the coldest day of the season.

†The coldest day of the season

‡The warmest day of the season

3.3 Summer: June – August

The downscaled scenarios for the summer season are summarized in Tables 7–8 and Figure 10. The skill of the empirical downscaling models for the summer is similar to the corresponding models for the winter and spring seasons. The station associated with a low R^2 value for the regression (weak relationship between the large-scale temperature and the local temperature) is the same as for the models for winter and spring. According to Table 2, the lowest temperature change estimate is negative, and is associated with a low R^2 -value (1%). The most important geographical factor is the distance from the coast (Table 8), but R^2 of the geographical model was only 0.10. The empirically downscaled temperature changes are in general weaker than the warming derived directly from the RCM results. In summer, there is no clear trend in the variance, and the change in the minimum daily temperatures is similar to those in the maximum daily temperatures.

TABLE 7. Same as Table 3, but for the summer season (June–August).

location	station no.	lon	lat	alt	R^2	p-value	ΔT	t-test	δ var	q95	q05
1 Røros	10400	11.38	62.57	628	75	0	0.96	0	0.97	0.90	1.57
2 Prestebakke	1130	11.54	58.99	157	16	0	0.33	0	1.13	0.60	0.36
3 Østre	11500	10.87	60.70	264	79	0	0.83	0	1.09	1.33	1.04
4 Lillehammer	12680	10.48	61.09	114	75	0	0.76	0	1.06	1.19	1.14
5 Venabu	13420	10.11	61.65	930	82	0	0.91	0	1.05	1.50	1.33
6 Skåbu	13670	9.38	61.52	890	68	0	0.77	0	1.08	1.34	1.02
7 Gjeilo	15540	8.45	61.87	378	73	0	0.75	0	1.03	1.14	1.15
8 Bråtå	15720	7.86	61.91	712	82	0	0.82	0	1.02	1.26	1.30
9 Fokstua	16610	9.29	62.11	386	81	0	0.94	0	0.99	1.09	1.30
10 Rygge	17150	10.79	59.38	205	69	0	0.88	0	0.98	0.92	0.79
11 Jøløy	17290	10.59	59.44	12	71	0	0.80	0	1.09	1.13	0.89
12 Oslo	18700	10.72	59.94	380	75	0	0.84	0	1.05	1.31	1.09
13 Tryvasshøgda	18960	10.69	59.99	528	80	0	1.10	0	1.08	1.68	1.59
14 Fornebu	19400	10.62	59.89	10	75	0	0.97	0	1.07	1.37	1.12
15 Dønski	19480	10.50	59.90	59	75	0	0.89	0	1.08	1.27	1.17
16 Asker	19710	10.44	59.86	163	6	0	-0.21	0	0.90	-0.19	0.01
17 Vest-torpa	21680	10.04	60.94	542	83	0	0.93	0	1.07	1.52	1.30
18 Fagernes	23420	9.24	60.99	365	78	0	0.76	0	1.06	1.44	0.94
19 Løken	23500	9.07	61.12	525	78	0	0.79	0	1.07	1.39	1.05
20 Nesbyen	24880	9.12	60.57	70	73	0	0.76	0	1.04	1.11	1.06
21 Geilo	25590	8.20	60.52	353	76	0	0.74	0	1.06	1.27	0.95
22 Finse	25840	7.50	60.60	1224	2	0	0.27	0	0.81	0.07	0.31
23 Måkerøy	27410	10.44	59.16	43	34	0	0.76	0	1.01	0.88	0.48
24 Færder	27500	10.53	59.03	6	71	0	0.87	0	0.96	0.91	0.76
25 Kongsberg	28370	9.65	59.66	168	76	0	0.95	0	1.07	1.45	1.32
26 Lungdal	28800	9.52	59.91	142	74	0	0.80	0	1.06	1.27	1.12
27 Magnor	2950	12.21	59.97	154	79	0	0.87	0	1.10	1.39	1.09
28 Møsstrand	31620	8.18	59.84	388	11	0	0.38	0	0.97	0.32	0.39
29 Lyngør	35860	9.15	58.63	4	64	0	0.82	0	0.98	0.83	0.66
30 Torungen	36200	8.79	58.38	12	60	0	0.79	0	0.96	0.73	0.71
31 Nelaug	36560	8.63	58.66	142	48	0	0.69	0	1.07	0.99	0.75
32 Tveitsund	37230	8.52	59.03	124	71	0	0.86	0	1.01	0.95	0.95
33 Landvik	38140	8.52	58.33	6	67	0	0.83	0	1.01	0.95	0.76
34 Kjevik	39040	8.07	58.20	23	62	0	0.83	0	0.96	0.78	0.68
35 Oksøy	39100	8.05	58.07	9	63	0	0.83	0	0.94	0.74	0.70
36 Byglandsfjord	39690	7.80	58.67	212	73	0	0.92	0	1.06	1.25	1.14
37 Lindesnes	41770	7.05	57.98	13	66	0	0.91	0	0.92	0.91	0.84
38 Lista	42160	6.57	58.11	14	64	0	0.95	0	0.91	0.83	0.96
39 Sirdal	42920	6.85	58.89	242	6	0	0.56	0	0.95	0.51	0.53
40 Ualand	43500	6.35	58.55	196	80	0	1.08	0	1.03	1.40	1.28
41 Obrestad	44080	5.56	58.66	24	55	0	0.84	0	0.88	0.70	0.88
42 Sola	44560	5.64	58.88	312	66	0	0.94	0	0.91	0.73	0.92
43 Suldal	46200	6.42	59.46	58	79	0	0.91	0	1.04	1.17	1.15
44 Midtlæger	46510	6.99	59.83	1079	30	0	0.77	0	1.05	1	0.88
45 Sauda	46610	6.36	59.65	240	76	0	0.79	0	1.04	1.24	0.81
46 Nedre	46910	5.75	59.48	64	78	0	1.03	0	1.01	1.24	1.12
47 Utsira	47300	4.88	59.31	55	62	0	0.91	0	0.88	0.67	0.96
48 Gardermoen	4780	11.08	60.21	202	80	0	0.88	0	1.09	1.42	1.17
49 Slåtterøy	48330	5.07	59.91	15	63	0	0.92	0	0.89	0.69	1.01

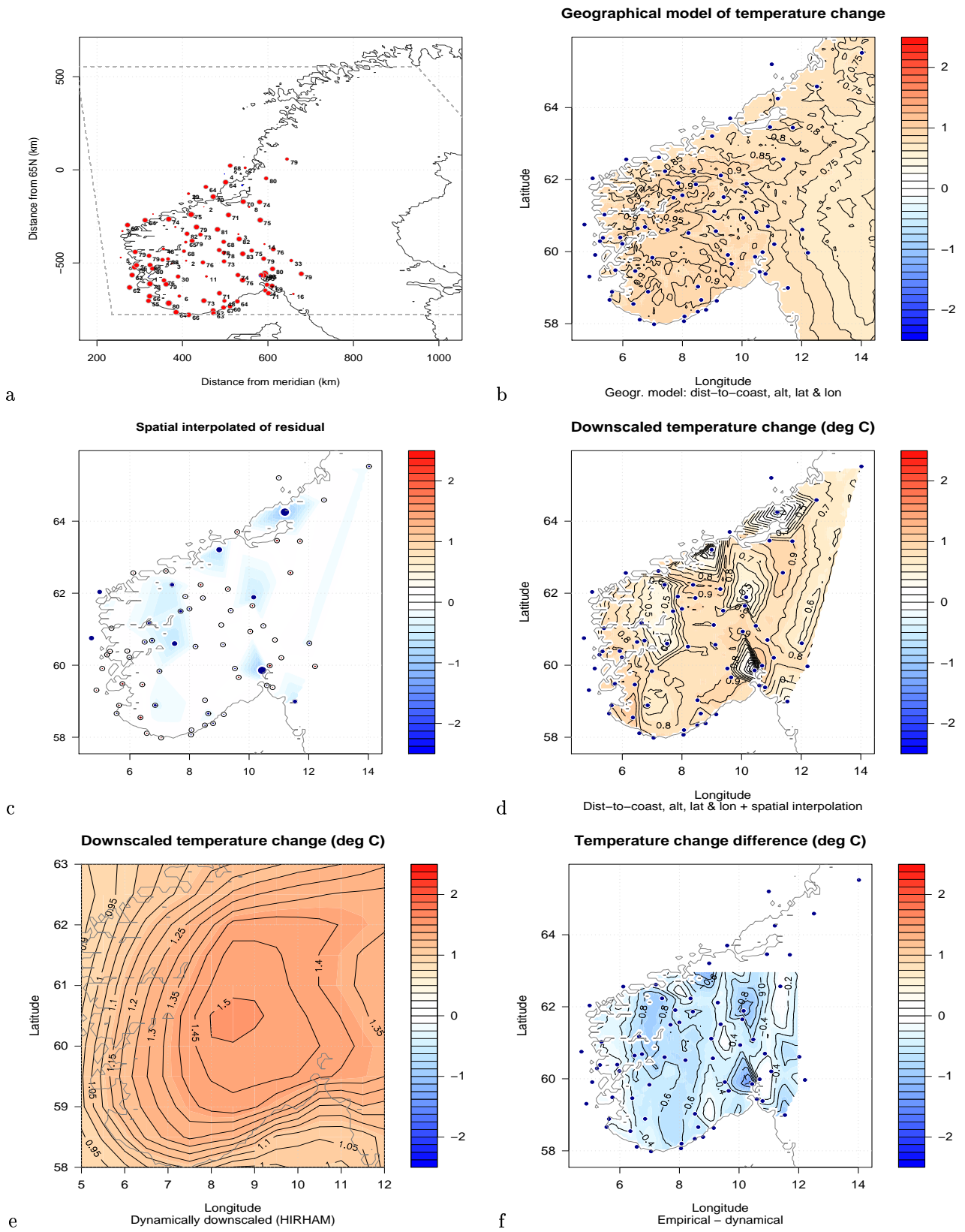


Figure 10. Same as in Figure 8, but for the summer season (June–August).

TABLE 7. Table continued...

	location	station no.	lon	lat	alt	R^2	p-value	ΔT	t-test	δ var	q95	q05
50	Upsangervatn	48390	5.77	59.84	60	1	0	-0.06	0	0.86	-0.03	0.02
51	Eidfjord	49580	6.86	60.47	165	3	0	0.26	0	1.02	0.37	0.28
52	Omastrand	50130	5.98	60.22	2	80	0	0.84	0	1.02	1.26	0.84
53	Kvamskogen	50300	5.91	60.39	210	80	0	0.85	0	1.03	1.26	0.83
54	Flesland	50500	5.23	60.29	48	75	0	0.97	0	0.96	1.17	1
55	Bergen	50540	5.33	60.38	23	76	0	0.91	0	0.98	0.90	0.89
56	Voss	51590	6.50	60.65	30	77	0	0.70	0	1.05	1.19	0.69
57	Reimegrend	51670	6.74	60.69	590	38	0	0.62	0	1.04	0.90	0.69
58	Modalen	52290	5.95	60.84	114	79	0	0.80	0	1.02	1.31	0.71
59	Hellisøy	52530	4.71	60.75	20	5	0	0.22	0	0.86	-0.03	0.05
60	Takle	52860	5.38	61.03	38	79	0	0.89	0	0.96	1.04	0.85
61	Vangsnes	53100	6.65	61.17	51	48	0	0.50	0	1	0.70	0.43
62	Lærdal	54130	7.52	61.06	36	68	0	0.64	0	1	0.93	0.90
63	Fortun	55160	7.70	61.50	27	65	0	0.48	0	0.99	0.70	0.60
64	Sognefjell	55290	8	61.57	1413	79	0	0.85	0	1.01	1.30	1.01
65	Kråkenes	59100	4.99	62.03	41	5	0	0.28	0	0.87	0.13	0.26
66	Svinøy	59800	5.27	62.33	38	62	0	0.88	0	0.86	0.58	0.89
67	Flisa	6040	12.02	60.61	184	33	0	0.57	0	1.05	0.82	0.63
68	Tafjord	60500	7.42	62.23	52	7	0	0.28	0	0.97	0.30	0.35
69	Vigra	60990	6.12	62.56	106	64	0	0.90	0	0.87	0.59	0.94
70	Hjelvik	61170	7.21	62.62	21	74	0	0.98	0	0.90	0.89	1.32
71	Lesjaskog	61770	8.37	62.23	621	79	0	0.97	0	0.99	0.97	1.55
72	Ona	62480	6.54	62.86	13	2	0	0.13	0	0.86	-0.01	0.12
73	Tingvoll	64550	8.30	62.84	69	75	0	1.07	0	0.91	0.93	1.63
74	Vinjeøra	65110	9	63.21	229	2	0	0.07	0	1.18	0.18	0.07
75	Sula	65940	8.47	63.85	5	29	0	0.45	0	0.83	0.29	0.59
76	Berkaak	66730	10.02	62.82	231	71	0	0.90	0	0.93	0.77	1.31
77	Selbu	68340	11.12	63.21	117	8	0	0.30	0	0.88	0.27	0.44
78	Vaernes	69100	10.94	63.46	23	70	0	0.94	0	0.85	0.49	1.40
79	Meråker	69330	11.70	63.44	145	74	0	0.88	0	0.90	0.83	1.45
80	Rena	7010	11.44	61.16	240	76	0	0.81	0	1.07	1.19	1.05
81	Ørland	71550	9.60	63.70	10	70	0	0.94	0	0.85	0.72	1.31
82	Halten	71850	9.41	64.17	16	64	0	0.75	0	0.85	0.47	0.91
83	Buholmråsa	71990	10.45	64.40	18	64	0	0.94	0	0.84	0.60	1.21
84	Namdalseid	72100	11.20	64.25	86	1	1	-0.31	0	0.91	-0.21	-0.13
85	Harran	73620	12.51	64.59	118	80	0	0.70	0	0.86	0.50	1.41
86	Nordøyen	75410	10.55	64.80	33	4	0	-0.06	0.04	0.95	-0.16	-0.19
87	Sklinna	75550	11	65.20	23	68	0	0.78	0	0.83	0.42	1.02
88	Leka	75600	11.70	65.10	47	27	0	0.45	0	0.85	0.31	0.77
89	Susendal	77750	14.02	65.52	265	79	0	0.58	0	0.84	0.48	1.28
90	Eyenstad	8130	11.14	61.41	255	14	0	0.24	0	0.99	0.41	0.36
91	Sørnesset	8710	10.15	61.89	739	3	0	0.22	0	0.89	0.23	0.35

TABLE 8. Same as Table 5, but for the summer season (June–August). [Residual standard error: 0.01283 on 74 degrees of freedom Multiple R-Squared: 0.09641, Adjusted R-squared: 0.02315 F-statistic: 1.316 on 6 and 74 DF, p-value: 0.2608].

	Estimate	Std. Error	t value	Pr(> t)
(Intercept)	1.24179392	0.78596513	1.58	0.12
dist	-0.07735636	0.05527924	-1.40	0.17
alt	0.00009259	0.00007252	1.28	0.21
lat	-0.00541998	0.01353266	-0.40	0.69
lon	-0.00656777	0.00979224	-0.67	0.51
grad.ns	0.00000243	0.00001395	0.17	0.86
grad.ew	-0.00001569	0.00001421	-1.10	0.27

3.4 Autumn: September – November

Tables 9–10 and Figure 11 give the downscaled results for the autumn. The stations with a weak relationship between the large-scale temperature structure and the local temperature are the same as in the other seasons. For four of the stations, the refined estimates indicate a slight cooling, and these stations were all associated with low downscaling skill scores: Asker ($R^2 = 0.06$) $\Delta T = -0.21^\circ\text{C}$; Upsangervatn ($R^2 = 0.01$) $\Delta T = -0.06^\circ\text{C}$; Namdalseid ($R^2 = 0.01$) $\Delta T = -0.31^\circ\text{C}$; Nordøyen ($R^2 = 0.04$) $\Delta T = -0.06^\circ\text{C}$. The empirical downscaling gives slightly weaker warming than the RCM on average, despite a higher

TABLE 9. Same as Table 3, but for the autumn season (September–November).

	location	station no.	lon	lat	alt	R^2	p-value	ΔT	t-test	δ var	q95	q05
1	Røros	10400	11.38	62.57	628	65	0	1.13	0	0.97	1.03	1.13
2	Prestebakke	1130	11.54	58.99	157	3	0	-0.08	0.01	0.76	-0.34	0
3	Østre	11500	10.87	60.70	264	70	0	1.08	0	1.04	1.16	0.63
4	Lillehammer	12680	10.48	61.09	114	64	0	1.01	0	1	1.04	0.82
5	Venabu	13420	10.11	61.65	930	63	0	0.94	0	1.02	1.12	0.65
6	Skåbu	13670	9.38	61.52	890	48	0	0.89	0	1.02	1.11	0.55
7	Gjeilo	15540	8.45	61.87	378	65	0	0.87	0	0.93	0.40	0.48
8	Bråtå	15720	7.86	61.91	712	64	0	0.69	0	0.96	0.37	0.15
9	Fokstua	16610	9.29	62.11	386	68	0	1.20	0	1.05	1.52	0.67
10	Rygge	17150	10.79	59.38	205	63	0	1.07	0	1.05	1.27	0.86
11	Jeløy	17290	10.59	59.44	12	60	0	0.71	0	1.03	0.68	0.36
12	Oslo	18700	10.72	59.94	380	61	0	1	0	1.07	1.23	0.77
13	Tryvasshøgda	18960	10.69	59.99	528	59	0	0.86	0	1.06	1	0.47
14	Fornebu	19400	10.62	59.89	10	60	0	1.01	0	1.07	1.23	0.97
15	Dønski	19480	10.50	59.90	59	57	0	1.01	0	1.08	1.29	1.02
16	Asker	19710	10.44	59.86	163	2	0	-0.07	0	0.82	-0.16	-0.01
17	Vest-torpa	21680	10.04	60.94	542	61	0	0.90	0	0.98	0.83	0.87
18	Fagernes	23420	9.24	60.99	365	60	0	0.78	0	0.95	0.56	0.85
19	Løken	23500	9.07	61.12	525	66	0	0.92	0	0.96	0.76	0.66
20	Nesbyen	24880	9.12	60.57	70	57	0	0.99	0	0.95	0.92	1.31
21	Geilo	25590	8.20	60.52	353	60	0	0.76	0	0.96	0.64	0.51
22	Finse	25840	7.50	60.60	1224	3	0	-0.10	0.01	0.83	-0.18	0.02
23	Måkerøy	27410	10.44	59.16	43	28	0	0.79	0	1.07	0.93	0.49
24	Færder	27500	10.53	59.03	6	64	0	0.70	0	1.04	0.75	0.40
25	Kongsberg	28370	9.65	59.66	168	60	0	1	0	1.02	1.10	0.95
26	Lungdal	28800	9.52	59.91	142	60	0	1.04	0	0.99	1.16	0.93
27	Magnor	2950	12.21	59.97	154	66	0	1.30	0	1.11	1.78	1.26
28	Møsstrand	31620	8.18	59.84	388	5	0	0.38	0	1.07	0.49	0.29
29	Lyngør	35860	9.15	58.63	4	62	0	0.69	0	0.99	0.63	0.61
30	Torungen	36200	8.79	58.38	12	63	0	0.69	0	1	0.67	0.59
31	Nelaug	36560	8.63	58.66	142	33	0	0.56	0	0.98	0.53	0.54
32	Tveitsund	37230	8.52	59.03	124	62	0	0.77	0	0.96	0.65	0.79
33	Landvik	38140	8.52	58.33	6	64	0	0.81	0	0.98	0.77	0.82
34	Kjevik	39040	8.07	58.20	23	59	0	0.69	0	0.94	0.53	0.85
35	Øksøy	39100	8.05	58.07	9	64	0	0.64	0	0.98	0.64	0.63
36	Byglandsfjord	39690	7.80	58.67	212	60	0	0.71	0	0.96	0.65	0.70
37	Listesnes	41770	7.05	57.98	13	68	0	0.65	0	1	0.66	0.53
38	Lista	42160	6.57	58.11	14	67	0	0.64	0	0.98	0.64	0.63
39	Sirdal	42920	6.85	58.89	242	3	0	-0.29	0	0.99	-0.13	-0.17
40	Ualand	43500	6.35	58.55	196	63	0	0.67	0	0.96	0.68	0.69
41	Obrestad	44080	5.56	58.66	24	69	0	0.69	0	0.98	0.77	0.62
42	Sola	44560	5.64	58.88	312	65	0	0.72	0	0.94	0.75	0.92
43	Suldal	46200	6.42	59.46	58	63	0	0.97	0	0.94	0.92	1.27
44	Midtlæger	46510	6.99	59.83	1079	16	0	-0.01	0.84	0.90	-0.07	-0.10
45	Sauda	46610	6.36	59.65	240	58	0	0.85	0	0.94	0.75	1.03
46	Nedre	46910	5.75	59.48	64	65	0	0.89	0	0.95	0.87	0.99
47	Utsira	47300	4.88	59.31	55	65	0	0.58	0	1.01	0.73	0.47
48	Gardermoen	4780	11.08	60.21	202	61	0	1.04	0	1.06	1.16	0.99
49	Slåtterøy	48330	5.07	59.91	15	64	0	0.63	0	0.99	0.73	0.63
50	Upsangervatn	48390	5.77	59.84	60	2	0	-0.34	0	1.01	-0.31	-0.26
51	Eidfjord	49580	6.86	60.47	165	7	0	0.57	0	1.17	0.78	0.53
52	Omastrand	50130	5.98	60.22	2	62	0	0.80	0	0.99	0.89	0.81
53	Kvamskogen	50300	5.91	60.39	210	64	0	0.92	0	0.99	1.08	0.96
54	Flesland	50500	5.23	60.29	48	69	0	0.85	0	0.99	1.03	0.91
55	Bergen	50540	5.33	60.38	23	65	0	0.81	0	0.97	0.92	0.92
56	Voss	51590	6.50	60.65	30	62	0	1	0	0.96	1.05	1.18
57	Reimegrend	51670	6.74	60.69	590	37	0	0.85	0	0.99	1.07	0.47
58	Modalen	52290	5.95	60.84	114	63	0	0.94	0	0.98	1.05	0.93
59	Hellisøy	52530	4.71	60.75	20	3	0	-0.09	0	0.84	-0.15	-0.04

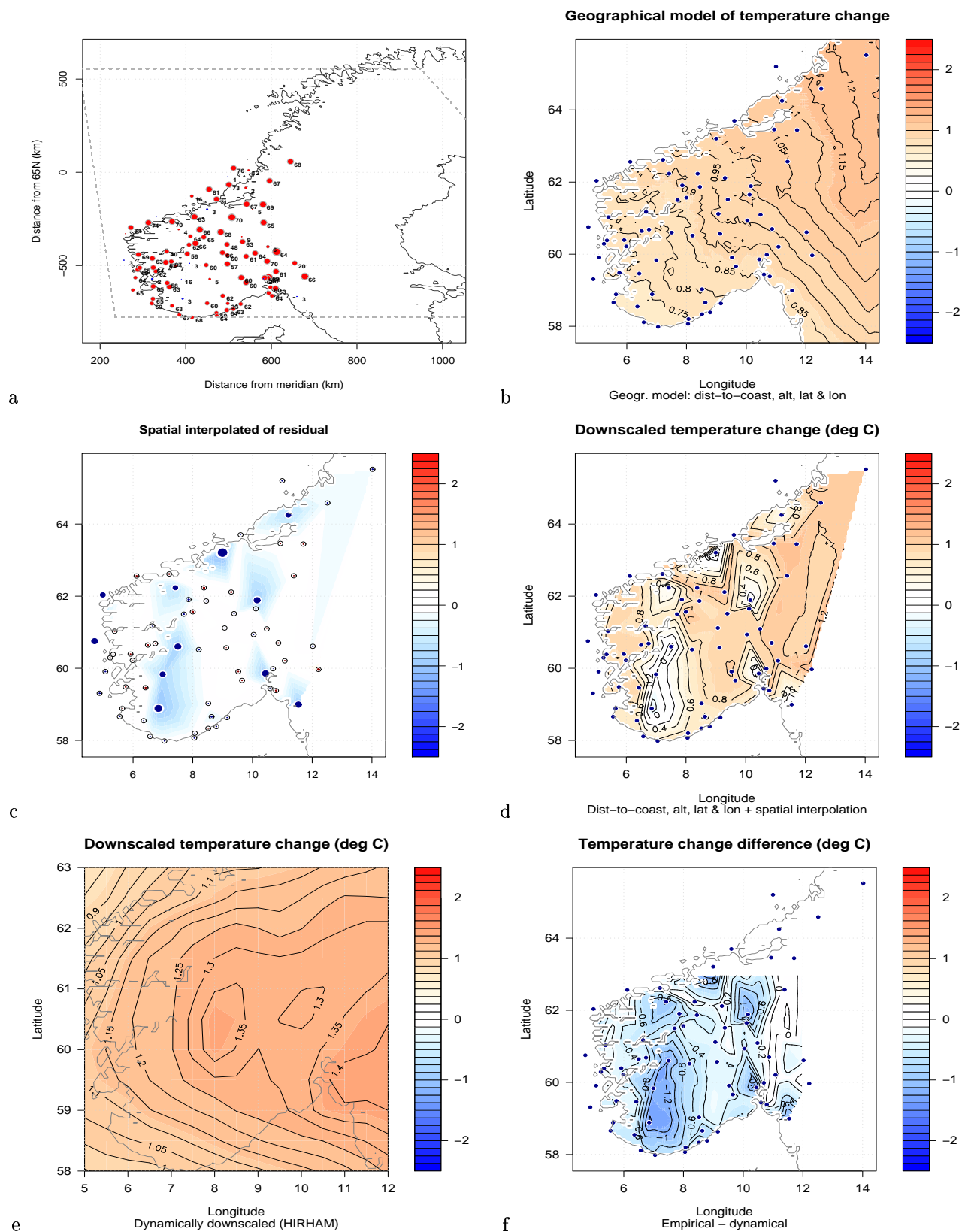


Figure 11. Same as in Figure 8, but for the autumn season (September–November).

TABLE 9. Table continued...

	location	station no.	lon	lat	alt	R^2	p-value	ΔT	t-test	δ var	q95	q05
60	Takle	52860	5.38	61.03	38	69	0	0.92	0	1.02	1.08	0.76
61	Vangsnes	53100	6.65	61.17	51	40	0	0.76	0	1.10	1	0.53
62	Lærdal	54130	7.52	61.06	36	56	0	0.91	0	0.95	0.80	1.08
63	Fortun	55160	7.70	61.50	27	62	0	0.77	0	0.96	0.54	0.66
64	Sognefjell	55290	8	61.57	1413	66	0	1.13	0	1.05	1.52	0.66
65	Kråkenes	59100	4.99	62.03	41	1	2	0.11	0	0.85	0.07	0.16
66	Svinøy	59800	5.27	62.33	38	71	0	0.94	0	1.11	1.28	0.69
67	Flisa	6040	12.02	60.61	184	20	0	0.88	0	1.11	1.19	0.57
68	Tafjord	60500	7.42	62.23	52	4	0	0.23	0	1	0.17	0.17
69	Vigra	60990	6.12	62.56	106	71	0	1.07	0	1.10	1.50	0.86
70	Hjelvik	61170	7.21	62.62	21	70	0	1.11	0	1.06	1.33	0.88
71	Lesjaskog	61770	8.37	62.23	621	66	0	1.18	0	0.98	1.18	0.84
72	Ona	62480	6.54	62.86	13	2	0	-0.02	0.09	0.75	-0.16	0.05
73	Tingvoll	64550	8.30	62.84	69	63	0	1.17	0	1.03	1.43	1.21
74	Vinjeøra	65110	9	63.21	229	3	0	-0.29	0	0.89	-0.37	-0.27
75	Sula	65940	8.47	63.85	5	16	0	0.54	0	1.22	0.82	0.36
76	Berkaak	66730	10.02	62.82	231	70	0	1.35	0	1.04	1.62	1.31
77	Selbu	68340	11.12	63.21	117	5	0	0.10	0.01	0.87	-0.03	0.22
78	Vaernes	69100	10.94	63.46	23	67	0	1.13	0	1.04	1.37	0.93
79	Meråker	69330	11.70	63.44	145	69	0	1.21	0	1.01	1.30	1.11
80	Rena	7010	11.44	61.16	240	64	0	1.47	0	1.08	2.02	1.17
81	Ørland	71550	9.60	63.70	10	71	0	1.03	0	1.09	1.17	1.02
82	Halten	71850	9.41	64.17	16	81	0	1.09	0	1.18	1.45	0.79
83	Buholmråsa	71990	10.45	64.40	18	73	0	1.08	0	1.14	1.32	0.69
84	Namdalseid	72100	11.20	64.25	86	2	0	0.36	0	1.12	0.37	0.33
85	Harran	73620	12.51	64.59	118	67	0	1.03	0	1.03	0.94	0.61
86	Nordøyen	75410	10.55	64.80	33	1	1	-0.01	0.38	0.86	-0.05	0.04
87	Sklinna	75550	11	65.20	23	76	0	0.99	0	1.15	1.28	0.56
88	Leka	75600	11.70	65.10	47	12	0	0.32	0	1.03	0.29	0.18
89	Susendal	77750	14.02	65.52	265	68	0	1.08	0	1.01	0.76	0.67
90	Evenstad	8130	11.14	61.41	255	6	0	0.52	0	0.98	0.52	0.26
91	Sørneset	8710	10.15	61.89	739	9	0	0.10	0.01	0.84	-0.07	0.30

TABLE 10. Same as Table 5, but for the autumn season (September–November). [Residual standard error: 0.01665 on 74 degrees of freedom Multiple R-Squared: 0.3756, Adjusted R-squared: 0.325 F-statistic: 7.42 on 6 and 74 DF, p-value: 3.08e-06] .

	Estimate	Std. Error	t value	Pr(> t)
(Intercept)	-2.19698523	0.94807339	-2.32	0.02
dist	0.05624505	0.07163566	0.79	0.44
alt	-0.00004343	0.00009503	-0.46	0.65
lat	0.04750664	0.01636640	2.90	0.01
lon	0.02186780	0.01246238	1.75	0.08
grad.ns	-0.00000016	0.00001780	-0.01	0.99
grad.ew	0.00000142	0.00001847	0.08	0.94

maximum value. For the geographical modelling, the strongest dependency appears to be associated with the latitude (Table 10), and the geographical model can account for 38% of the spatial variance. There is no clear decrease in the future variance associated with the daily mean temperature, and the maximum and minimum daily temperature warm at approximately same rate.

3.5 Best estimates

The analysis so far has regarded the residuals from all stations equivalently. Although the differences in downscaling skill-scores are taken into account as weights in the geographical model, the small group of stations with a low downscaling skill-scores (that give unrealistic results) produce spurious features in the maps derived from the sum of the geographical model and the interpolated residuals. Hence, the interpolation of the residuals is repeated where only stations with high downscaling skill-scores ($R^2 > 0.5$) are included. These new maps, shown in Figure 12 provide more realistic scenarios. The differences between these new improved maps and the output from the RCM are shown in Figure 13. By excluding the “bad” stations, the results from the empirical downscaling become more similar in

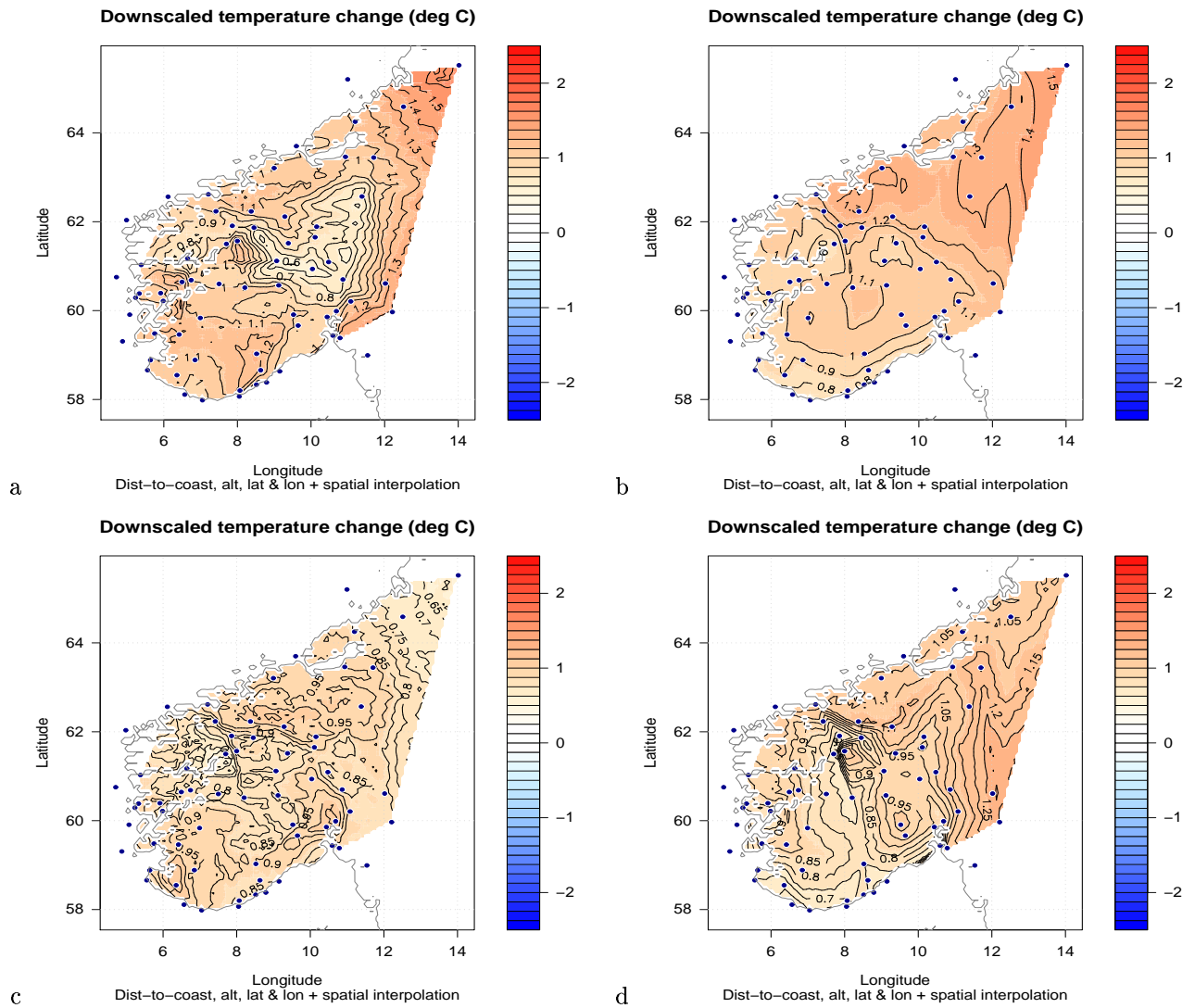


Figure 12. The best-estimate for the temperature scenario derived only taking into account the residuals of downscaled scenarios associated with $R^2 > 0.5$, for winter (a), spring (b), summer (c), and autumn (d).

magnitude to the RCM results. However, the empirically-based refinement of the RCM output yields generally weaker warming for the winter, summer and autumn seasons and somewhat stronger warming during spring. Local geographical features are also still more pronounced in the improved analysis.

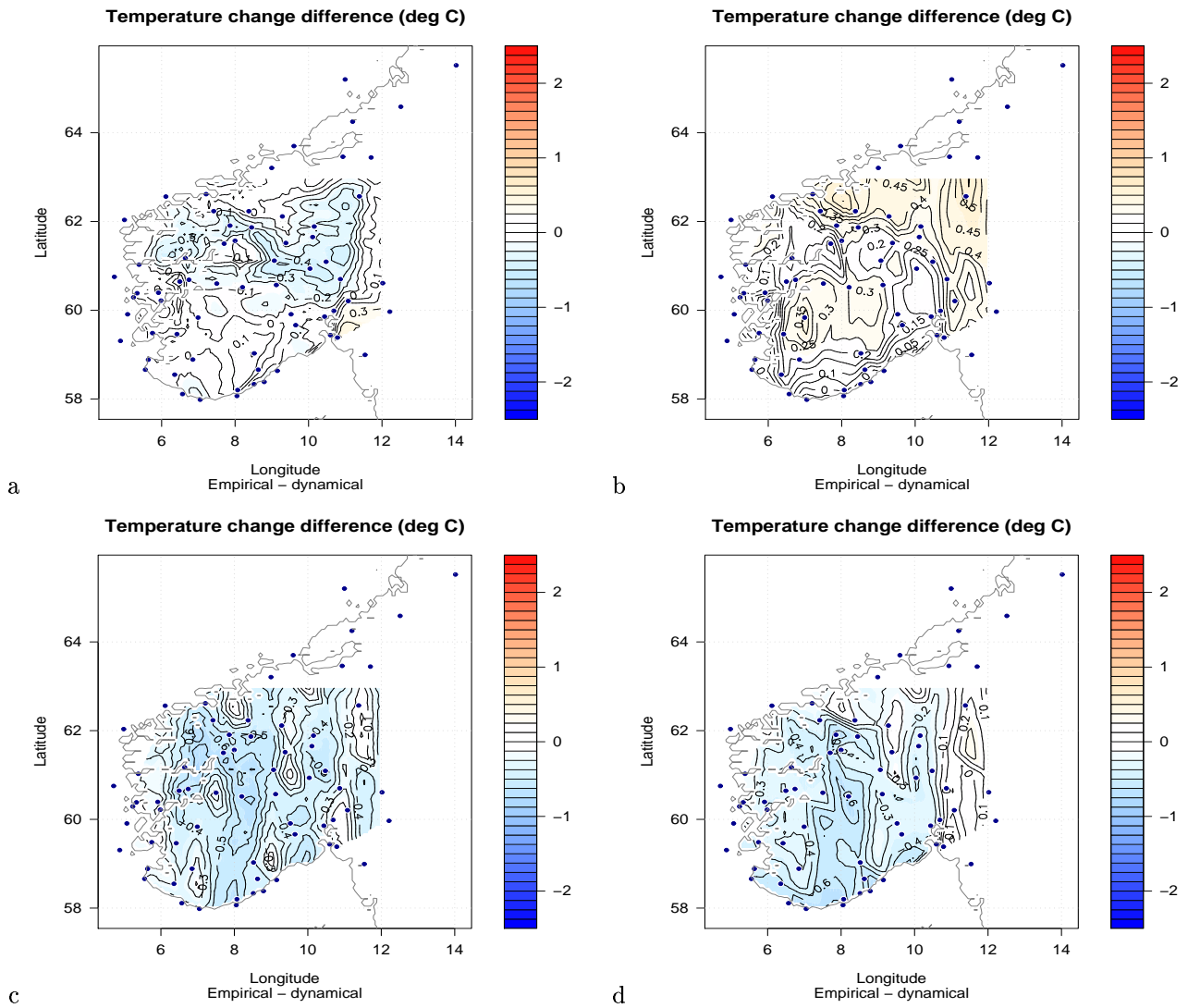


Figure 13. The difference between the best-estimate scenarios in Figure 12 and the purely dynamically down-scaled results from HIRHAM.

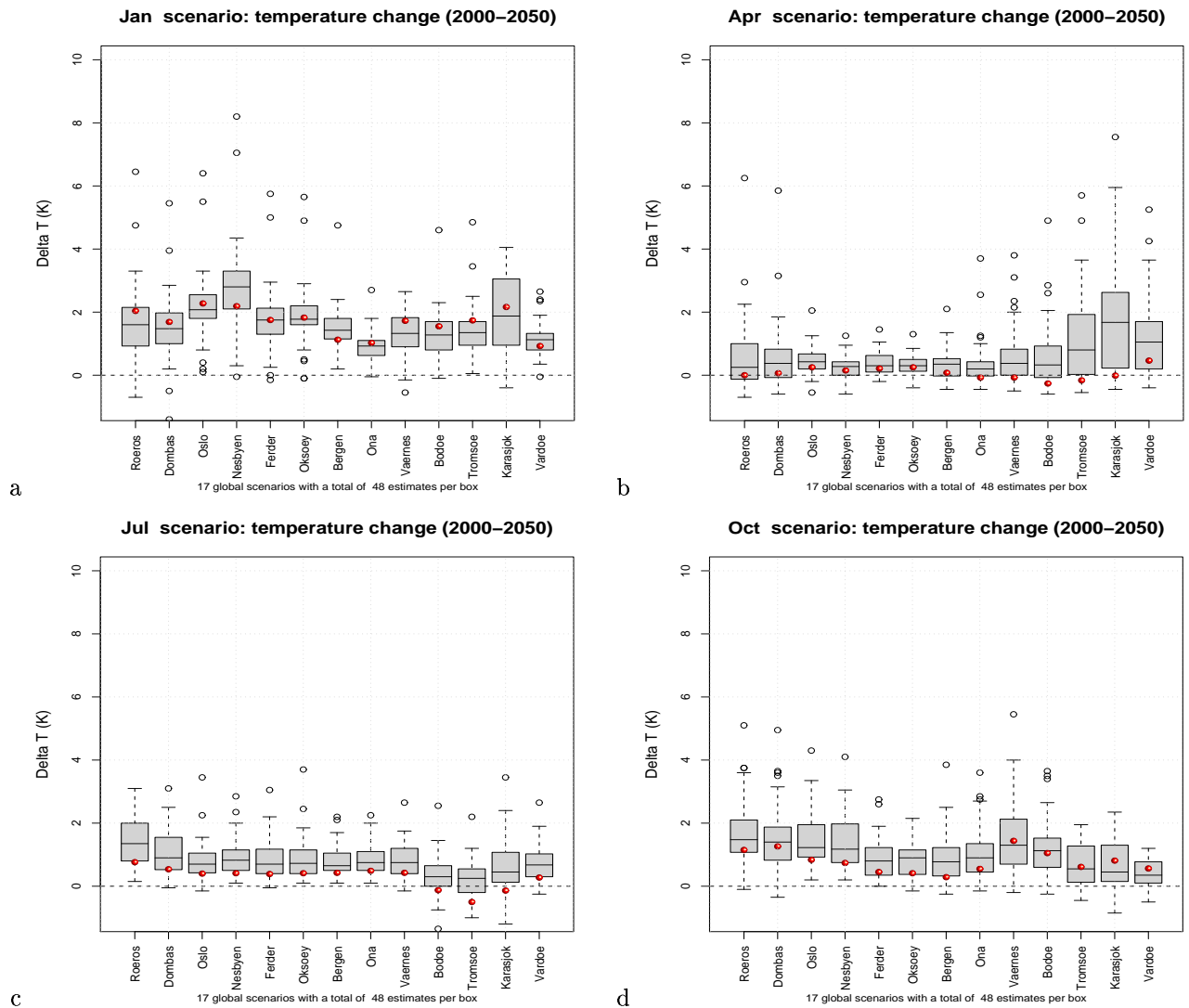


Figure 14. A comparison between estimated temperature change over the interval 2000-2050 derived from the ECHAM4/OPYC3 GSDIO integration and a multi-model GCM ensemble described in *Benestad* (2002a). The red balls indicate the mean value of four downscaled estimates from the ECHAM4/OPYC3 GSDIO using T(2m) fields as predictor.

4 Discussion and conclusion

The objective of this study has been to investigate the possibility of refining the description of local climatic changes, given a dynamically downscaled scenario. The analysis indicates that an empirically-based refinement yields quite different results than the original HIRHAM scenarios. The high skill (R^2 and p-values in Table 3) suggests that the empirical downscaling models are appropriate for most locations, however, the empirical models fail for a small group of stations. The geographical model used for spatial interpolation gives a simple picture of the local climate away from these locations, but this model is not perfect. Nevertheless, the model is believed to produce a fairly credible description of the climate, and is therefore useful for producing scenarios as these merely represent plausible descriptions of the future.

The comparison between the refined scenarios and the HIRHAM results indicate the presence of uncertainties in the analyses, as do the RCM shortcomings reported by *Skaugen et al.* (2002). However, it is important to keep in mind that the main uncertainties are probably due to AOGCM shortcomings and statistical fluctuations associated with internal variability (*Benestad, 2002a*). The uncertainties

TABLE 11. A comparison between the variance of January temperatures from the daily station records and corresponding interpolated values from the ERA-15 data. The spatial interpolation used a bilinear scheme (the R-package 'akima').

	lon./lat., alt.	var(obs)	var(ERA)
Flisa	12.02E/60.61N, 184m a.s.l	93.31,	36.83
Lillehammer	10.47E/61.1N, 239m a.s.l	79.75,	57.19
Fokstua	9.28E/62.12N, 972m a.s.l	60.3,	46.17
Rygge	10.78E/59.38N, 40m a.s.l	65.08,	39.03
Oslo	10.71E/59.95N, 94m a.s.l	67.31,	42.5
Geilo	8.2E/60.52N, 810m a.s.l	63.59,	43.24
Lungdal	9.52E/59.9N, 288m a.s.l	77.56,	52.3
Tveitsund	8.52E/59.03N, 252m a.s.l	60.36,	50.61
Sirdal	6.15E/58.88N, 500m a.s.l	56.02,	24.37
Sola	5.63E/58.88N, 7m a.s.l	32.97,	17.92
Voss	6.5E/60.65N, 125m a.s.l	60.52,	20.13
Tafjord	7.42E/62.23N, 15m a.s.l	36.44,	33.54
Selbu	11.12E/63.2N, 242m a.s.l	54.14,	46.23
Susendal	14.02E/65.52N, 265m a.s.l	85.36,	31.5
Glomfjord	13.98E/66.82N, 39m a.s.l	37.85,	37.51
Sortland	15.42E/68.7N, 3m a.s.l	36.85,	50.06
Tennevoll	17.8E/68.73N, 22m a.s.l	68.62,	59.27
Bardufoss	18.53E/69.06N, 76m a.s.l	93.72,	57.66
Tromsø	18.93E/69.65N, 100m a.s.l	44.35,	73.51
Nordreisa	21.02E/69.73N, 1m a.s.l	76.54,	54.74
Nordstraum	21.88E/69.83N, 6m a.s.l	47.05,	39.75
Alta	23.35E/69.98N, 3m a.s.l	78.82,	12.1
Suolovuopmi	23.52E/69.33N, 374m a.s.l	112.53,	7.17

are further increased with dynamical downscaling (*Christensen et al., 2001*), empirical downscaling (*Benestad, 2001*), geographical model, and natural variability (e.g. volcanos and solar activity).

Skaugen et al. (2002) argue that the correction $T' = aT + b$ results in too low estimate using since they found $a < 0$ for all stations, which also implies that R^2 values less than 100% will under-estimate the warming. It is possible that this is more of a problem for $R^2 < 100\%$, as the value in a may also reflect amplitude differences between local temperature and interpolations from ERA-15 (Table 11). A regression between gridded and local temperatures is expected to yield variance of nearly 100%, and low R^2 values indicate the presence of errors in the re-analysis or the station records. This way, the empirical downscaling analysis may give conservative trend estimates. A technique called “inflation” *von Storch (1999)* that forces similar variance has sometimes been used, but this kind of re-scaling is not a good solution because an R^2 value lower than 100% means that the predictor cannot account for all of the change and that other factors may play a role. One could argue, however, that the downscaled trend estimates are conservative and represent the lower end of a plausible range, and that the upper end should be the trend-estimate scaled by $1/R^2$. Non-normalities may also reduce the skill of the empirical downscaling models. Analog models or transformations can be employed in order to predict the right level of variance. The classical analog models are, however, not capable of projecting new record values. A simple height-correction $T' = T + b$ for the temperature has been proposed by *Skaugen et al. (2002)* as a good solution for describing the local temperature distributions, but this kind of correction does not take into account potential altitude-dependencies of the temperature change. Tables 1, 5, 6, 8, and 10 do suggest that the projected warming does not depend strongly on the altitude, thus justifying the simple height-correction. Another caveat may be that using single grid-box values from GCMs is not recommended since they may have lower limit of skillful spatial scale (*von Storch et al., 1993b*) of ~ 8 grid-boxes (*Grotch & MacCracken, 1991*). This kind of limitation may also apply to RCMs.

It has been shown that the empirically downscaled results may also be sensitive to the choice of method and predictor (*Benestad, 2001, 2000; Huth, 2002*). An implicit assumption of empirical downscaling is that the relationship between the large-scale and local climate is stationary (*Wilby, 1997*). Although this condition can be tested for the past (*Benestad, 2001*), one cannot be certain that this condition will hold for the future. The problem of non-stationarity also applies to the general circulation models that incorporates so-called ‘parameterisation schemes’, i.e. statistical description of sub-grid processes.

It is important to keep in mind the limitations of using only one climate scenario based on just one GCM. Not only do integrations with different climate models give different results, but different initial conditions and various ways of describing how clouds are affected by a climate change also give

rise to different results (*Benestad, 2002a*). It is therefore desirable to have an idea of how the results of GSDIO compares with others. Figure 14 shows box-and-whisker plots of estimated temperature change over 2000–2050 for a multi-model ensemble for a selection of Norwegian locations and for four different months. These estimates were derived through empirical downscaling, and the methodology and the results are discussed in detail by *Benestad (2002a)*. The red balls indicate the magnitude of the warming estimated by the GSDIO model. In January, the GSDIO-based results are mainly within the multi-model ensemble without any systematic bias with respect to the other models. In April and July, on the other hand, the GSDIO results give systematically weaker warming than the majority of the GCMs in the ensemble, and in the autumn it is only in the north that the downscaled GSDIO results are greater than the multi-model median.

Acknowledgments: This work was done under the Norwegian Regional Climate Development under Global Warming (RegClim) programme, and was supported by the Norwegian Research Council (Contract NRC-No. 120656/720) and the Norwegian Meteorological Institute. Jan Erik Haugen and Dag Bjørge produced, prepared and provided the results from the RegClim dynamical downscaling and Torill Engen Skaugen prepared the daily temperature and precipitation data. The analysis was carried out using the R (*Ellner, 2001; Gentleman & Ihaka, 2000*) data processing and analysis language, which is freely available over the Internet (URL <http://www.R-project.org/>).

References

- Beckmann, B.-R., & Buishand, T.A., 2002. Statistical downscaling relationships for precipitation in the Netherlands and north Germany. *International Journal of Climatology*, **22**, 15–32.
- Benestad, R.E., 2000. *Future Climate Scenarios for Norway based on linear empirical downscaling and inferred directly from AOGCM results*. KLIMA 23/00. DNMI, PO Box 43 Blindern, 0313 Oslo, Norway.
- Benestad, R.E., 2001. A comparison between two empirical downscaling strategies. *Int. J. Climatology*, **21**, 1645–1668. DOI 10.1002/joc.703.
- Benestad, R.E., 2002a. Empirically downscaled multi-model ensemble temperature and precipitation scenarios for Norway. *Journal of Climate*, **15**, 3008–3027.
- Benestad, R.E., 2002b. Empirically downscaled temperature scenarios for northern Europe based on a multi-model ensemble. *Climate Research*, **21**, 105–125.
- Benestad, R.E., 2003a. *clim.pact-V.1.0*. KLIMA 04/03. The Norwegian Meteorological Institute, PO Box 43 Blindern, 0313 Oslo, Norway.
- Benestad, R.E., 2003b. *Downscaling analysis for daily and monthly values using clim.pact-V.0.9*. KLIMA 01/03. met.no, PO Box 43 Blindern, 0313 Oslo, Norway.
- Benestad, R.E., Hanssen-Bauer, I., & Førland, E.J., 2002. Empirically downscaled temperature scenarios for Svalbard. *Atmospheric Science Letters*, September 18, doi.10.1006/asle.2002.0051.
- Bjørge, D., & Haugen, J.E., 1999. PT1: Simulation of present-day climate in HIRLAM using 'perfect' boundaries. *Pages 9–16 of: Iversen, T., & Høiskar, B.A.K. (eds), RegClim*. General Technical report, nos. 2PT1: HIRHAM simulation with high NAO-index MPI boundary data, present-day and scenario climate. <http://www.nilu.no/regclim/>: NILU.
- Bjørge, D., Haugen, J.E., & Nordeng, T.E., 2000. *Future Climate in Norway*. Research Report 103. DNMI, PO Box 43 Blindern, 0313 Oslo, Norway.
- Charles, SP, Bates, BC, Whetton, PH, & Hughes, JP., 1999. Validation of downscaling models for changed climate conditions: case study of southwestern Australia. *Climate Research*, **12**(June), 1–14.
- Christensen, J.H., Risnen, J., Iversen, T., Bjørge, D., Christensen, O. B., & Rummukainen., 2001. A synthesis of regional climate change simulations - A Scandinavian perspective. *Geophys. Res. Lett.*, **28**(6), 1003.
- Christensen, O.B., J.H., Christensen, Machenhauer, B., & Botzet, M., 1998. Very High-Resolution Climate Simulations over Scandinavia - Present Climate. *Journal of Climate*, **11**, 3204–3229.
- Easterling, D.R., 1999. Development of regional climate scenarios using a downscaling approach. *Climatic Change*, **41**, 615–634.
- Ellner, S.P., 2001. Review of R, Version 1.1.1. *Bulletin of the Ecological Society of America*, **82**(April), 127–128.
- Gentleman, R., & Ihaka, R., 2000. Lexical Scope and Statistical Computing. *Journal of Computational and Graphical Statistics*, **9**, 491–508.
- Gibson, J. K., Kallberg, P., Uppala, S., Hernandez, A., Nomura, A., & Serrano, E., 1997. *ERA Description*. ERA Project Report Series. ECMWF.
- Goodess, C.M., & Palutikof, J.P., 1998. Development of daily rainfall scenarios for southeast Spain using a circulation-type approach to downscaling. *International Journal of Climatology*, **10**, 1051–1083.
- Grotch, S., & MacCracken, M., 1991. The use of general circulation models to predict regional climate change. *Journal of Climate*, **4**, 286–303.
- Hanssen-Bauer, I., Tveito, O.E., & Førland, E.J., 2000. *Temperature Scenarios for Norway*. KLIMA 24/00. DNMI, PO Box 43 Blindern, 0313 Oslo, Norway.
- Hanssen-Bauer, I., Frland, E.J., Haugen, J.E., & Tveito, O.E., 2003. Temperature and precipitation scenarios for Norway: Comparison of results from dynamical and empirical downscaling. *Climate Research*, **accepted**.
- Haugen, J.E., Bjørge, D., & Nordeng, T.E., 1999a. A 20-year climate change experiment with HIRHAM, using MPI boundary data. *Pages 37–44 of: Iversen, T., & Høiskar, B.A.K. (eds), RegClim*. General Technical report, no. 3. <http://www.nilu.no/regclim/>: NILU.
- Haugen, J.E., Bjørge, D., & Nordeng, T.E., 1999b. PT1: HIRHAM simulation with high NAO-index MPI boundary data, present-day and scenario climate. *Pages 145–152 of: Iversen, T., & Høiskar, B.A.K. (eds), RegClim*. General Technical report, no. 2. <http://www.nilu.no/regclim/>: NILU.
- Haugen, J.E., Bjørge, D., & Nordeng, T.E., 2000. Dynamical downscaling PT1: Further results. *Pages 79–82 of: Iversen, T., & Høiskar, B.A.K. (eds), RegClim*. General Technical report, no. 4.

- <http://www.nilu.no/regclim/>: NILU.
- Hellström, C., Chen, D., Achberger, C., & Räisänen, J., 2001. Comparison of climate change scenarios for Sweden based on statistical and dynamical downscaling of monthly precipitation. *Climate Research*, **19**, 45–55.
- Heyen, H., Zorita, E., & von Storch, H., 1996. Statistical downscaling of monthly mean North Atlantic air-pressure to sea level anomalies in the Baltic Sea. *Tellus*, **48A**, 312–323.
- Huth, R., 2002. Statistical Downscaling of Daily Temperature in Central Europe. *Journal of Climate*, **15**, 1731–1742.
- IPCC., 1995. *The Second Assessment Report*. Technical Summary. WMO & UNEP.
- IPCC., 2001. *IPCC WGI THIRD ASSESSMENT REPORT*. Summary for Policymakers. WMO.
- Jones, P. D., Raper, S. C. B., Bradley, R. S., Diaz, H. F., Kelly, P. M., & Wigley, T. M. L., 1998. Northern Hemisphere surface air temperature variations, 1851–1984. *J. Clim. Appl. Met.*, **25**, 161–179.
- Kidson, J.W., & Thompson, C.S., 1998. A Comparison of Statistical and Model-Based Downscaling Techniques for Estimating Local Climate Variations. *Journal of Climate*, **11**, 735–753.
- Murphy, J., 1999. An Evaluation of Statistical and Dynamical Techniques for Downscaling Local Climate. *Journal of Climate*, **12**, 2256–2284.
- Murphy, J., 2000. Predictions of climate change over Europe using statistical and dynamical downscaling techniques. *International Journal of Climatology*, **20**, 489–501.
- Nordeng, T.E., Haugen, J.E., & Bjørge, D., 2000. Dynamical downscaling - further work in RegClim. Pages 29–32 of: Iversen, T., & Høiskar, B.A.K. (eds), *RegClim*. General Technical report, no. 5. <http://www.nilu.no/regclim/>: NILU.
- Oberhuber, J.M., 1993. Simulation of the Atlantic circulation with a coupled sea ice-mixed layer isopycnal general circulation model. Part 1: Model description. *Journal of Physical Oceanography*, **22**, 808–829.
- Oshima, N., Kato, H., & Kadokura, S., 2002. An application of statistical downscaling to estimate surface air temperature in Japan. *Journal of Geophysical Research*, **107**(D10), ACL–14.
- Prudhomme, C., & Reed, D., 1999. Mapping extreme rainfall in a mountainous region using geostatistical techniques: A case study in Scotland. *International Journal of Climatology*, **19**, 1337–1356.
- Räisänen, J., Rummukainen, M., Ullerstig, A., Bringfelt, B., Hansson, U., & Willén, U., 1999 (Feb.). *The first Rossby Centre Regional Climate Scenario - Dynamical Downscaling of CO₂-induced Climate Change in the HadCM2 GCM*. SWECLIM 85. SMHI.
- Roeckner, E., Arpe, K., Bengtsson, L., Dümenil, L., Esch, M., Kirk, E., Lunkeit, F., Ponater, M., Rockel, B., Sausen, B., Schlese, U., Schubert, S., & Windelband, M., 1992. *Simulation of present-day climate with the ECHAM model: impact of model physics and resolution*. Tech. rept. 93. Max Planck-Institute für Meteorologie, Hamburg.
- Schubert, S., 1998. Downscaling local extreme temperature change in south-eastern Australia from the CSIRO MARK2 GCM. *International Journal of Climatology*, **18**, 1419–1438.
- Skaugen, T.E., Hanssen-Bauer, I., & Førland, E.J., 2002. *Adjustment of dynamically downscaled temperature and precipitation data in Norway*. KLIMA 20/02. The Norwegian Meteorological Institute, PO Box 43 Blindern, 0313 Oslo, Norway.
- Tveito, O.E., & Førland, E.J., 1999. Mapping temperatures in Norway applying terrain information, geostatistics and GIS. *Norsk geografisk tidsskrift*, **53**, 202–212.
- von Storch, H., 1999. On the Use of "Inflation" in Statistical Downscaling. *Journal of Climate*, **12**, 3505–3506.
- von Storch, H., Zorita, E., & Cubasch, U., 1993a. Downscaling of Global Climate Change Estimates to Regional Scales: An Application to Iberian Rainfall in Wintertime. *Journal of Climate*, **6**, 1161–1171.
- von Storch, H., Zorita, E., & Cubasch, U., 1993b. Downscaling of Global Climate Change Estimates to Regional Scales: An Application to Iberian Rainfall in Wintertime. *Journal of Climate*, **6**, 1161–1171.
- Wilby, R.L., 1997. Non-stationarity in daily precipitation series: Implications for GCM down-scaling using atmospheric circulation indices. *International Journal of Climatology*, **17**, 439–454.
- Wilby, R.L., & Wigley, T.M.L., 2000. Precipitation predictors for downscaling: Observed and general circulation model relationships. *International Journal of Climatology*, **20**, 641–661.
- Wilby, R.L., Wigley, T.M.L., Conway, D., Jones, P.D., Hewitson, B.C., Main, J., & Wilks, D.S., 1998a. Statistical downscaling of general circulation model output: a comparison of methods. *Water Resources Research*, **34**, 2995–3008.
- Wilby, R.L., Hassan, H., & Hanaki, Keisuke., 1998b. Statistical downscaling of hydrometeorological

- variables using general circulation model output. *Journal of Hydrology*, **205**, 1–19.
- Wilks, D.S., 1995. *Statistical Methods in the Atmospheric Sciences*. Orlando, Florida, USA: Academic Press.
- Zorita, E., & von Storch, H., 1999. The Analog Method as a Simple Statistical Downscaling Technique: Comparison with More Complicated Methods. *Journal of Climate*, **12**, 2474–2489.